

Groundhog: Efficient Request Isolation in FaaS

Mohamed Alzayat Jonathan Mace Peter Druschel Deepak Garg
{alzayat,jcmace,druschel,dg}@mpi-sws.org
Max Planck Institute for Software Systems (MPI-SWS)
Saarbruecken, Saarland, Germany

Abstract

Security is a core responsibility for Function-as-a-Service (FaaS) providers. The prevailing approach has each function execute in its own container to isolate concurrent executions of different functions. However, successive invocations of the same function commonly reuse the runtime state of a previous invocation in order to avoid container cold-start delays when invoking a function. Although efficient, this container reuse has security implications for functions that are invoked on behalf of differently privileged users or administrative domains: bugs in a function’s implementation, third-party library, or the language runtime may leak private data from one invocation of the function to subsequent invocations of the same function.

Groundhog isolates sequential invocations of a function by efficiently reverting to a clean state, free from any private data, after each invocation. The system exploits two properties of typical FaaS platforms: each container executes at most one function at a time and legitimate functions do not retain state across invocations. This enables Groundhog to efficiently snapshot and restore function state between invocations in a manner that is independent of the programming language/runtime and does not require any changes to existing functions, libraries, language runtimes, or OS kernels. We describe the design of Groundhog and its implementation in OpenWhisk, a popular production-grade open-source FaaS framework. On three existing benchmark suites, Groundhog isolates sequential invocations with modest overhead on end-to-end latency (median: 1.5%, 95p: 7%) and throughput (median: 2.5%, 95p: 49.6%), relative to an insecure baseline that reuses the container and runtime state.

1 Introduction

Function-as-a-Service (FaaS) is an emerging high-level abstraction for cloud applications. Tenants state their application logic as a function implementation written in a high-level language like Python or JavaScript. The FaaS provider in turn exports an HTTP/S endpoint, which can be used to invoke the function with arguments and receive results. The FaaS provider is responsible for deploying and executing the tenants’ functions, provisioning and scaling resources as workload demand fluctuates, and maintaining and multiplexing the hardware and software infrastructure across different tenants and functions. FaaS has an ‘on-demand’ payment model: a tenant only pays for the compute time used to execute their functions.

Among the core responsibilities of a FaaS provider is security. For scalability and efficiency, FaaS platforms multiplex

functions of different tenants concurrently on a large pool of shared resources. FaaS platforms rely on various language-, process-, and VMM-based isolation mechanisms to isolate functions from one another: each function executes within its own execution environment and *different functions* do not share the same execution environment. *Container isolation* is a commonly-used, general, low-entry-barrier function isolation mechanism that relies on standard OS process-isolation primitives. An alternative to container isolation is VMM-based isolation, where each function executes in a separate VM. Both container and VMM-based isolation prevent a malicious or compromised function from affecting the availability, integrity, and confidentiality of other functions.

So far, the focus of security in FaaS has been on isolating *different functions* from each other. However, ideally, a FaaS platform should provide the same degree of isolation among *sequential activations of the same function*; otherwise, bugs in a function implementation — or a third-party library / runtime it depends on — may cause a leak of information from one activation of a function to a subsequent one. This *sequential request isolation* is critical if a function can be invoked by, or on behalf of, differently privileged callers, such as unrelated end-clients of a service built on top of the function. For example, if the same function container is first invoked to service Alice’s request and then invoked again to service Bob’s request, there is a possibility that a bug in the function, some library or the language runtime causes some of Alice’s data from the first request to be retained and later leaked into the response returned to Bob. It is this sequential request isolation problem that we focus on in this paper.

A trivial way to attain sequential request isolation would be to run not just every function but also *every activation of a function* in a freshly initialized container. However, this solution is problematic from the perspective of performance: Container initialization overheads are high, ranging from a few seconds when done naively to hundreds of milliseconds with existing solutions to reduce the cost of container cold-starts [5, 9, 16, 20, 34, 42, 45, 50], which is higher than the basic execution time of a significant fraction of FaaS functions (e.g., [39] report function execution times in Microsoft Azure, with a median of 900 ms and a 25th %-ile of 100 ms and we observe even lower function execution times in our experimental setup). Hence, this trivial solution to sequential request isolation would impose impractical overhead.

This paper presents Groundhog, a system that adds lightweight sequential request isolation to a FaaS framework that

already uses containers to isolate different functions. Importantly, Groundhog reuses containers across requests to the same function, thus avoiding the per-activation container re-initialization cost of the trivial solution above.¹ Groundhog is independent of the language, runtime, or libraries used to implement functions, does not require changes to function implementations, OS kernels or hypervisors, and preserves most of the performance benefits of container reuse. To the best of our knowledge, Groundhog is the first system to do so.

Groundhog exploits two properties of FaaS platforms to enable a general-purpose, lightweight, performant solution: (1) At most one function activation executes at any time in a container; and (2) functions are not expected to retain runtime state across activations. Accordingly, the core of Groundhog’s sequential request isolation is a general, in-memory, *lightweight process snapshot/restore* mechanism. Groundhog encapsulates each function in a (containerized) process, and takes a snapshot of each function process’ fully initialized state, just before the function is being invoked for the first time. While this state typically includes a fully initialized language runtime including multiple threads, the function has not yet received activation-specific arguments or credentials, and its state is therefore guaranteed to be free of secrets. Subsequently, whenever the function has finished an activation and returned its results, Groundhog restores the function’s process to the clean state recorded in the snapshot.

Groundhog is secure because the restoration ensures that no data can leak from one activation to a subsequent one. Groundhog is efficient because the cost of restoring state is roughly proportional to the amount of memory modified during an activation. As we will show, most function activations modify only a small proportion of the function process’ total state. Finally, Groundhog restores state *between activations of a function*, and therefore does not contribute to a function’s activation latency under low to medium server load.

We have implemented Groundhog in C using commodity Linux kernel features. We evaluate Groundhog in OpenWhisk using Python, Node.js, and C functions from the FaaSProfiler benchmark [38], pyperformance [48] and PolyBench [30] benchmarks, which cover a wide variety of use cases. We demonstrate that Groundhog achieves sequential request isolation with modest overhead on end-to-end latency (median: 1.5%, 95p: 7%) and throughput (median: 2.5%, 95p: 49.6%) relative to an insecure baseline that reuses containers and runtimes. The main contributions of this paper include:

- ① The design of a language and runtime-independent, in-memory *lightweight process snapshot/restore* mechanism for achieving general-purpose sequential request isolation in FaaS while retaining the performance benefits of container reuse.
- ② The design and implementation of Groundhog², a system

¹We describe our work in the context of FaaS platforms that already use containers to isolate different functions from each other, but similar design principles should apply to VMM-based isolation.

²The implementation will be open-sourced after the paper’s publication.

that provides lightweight sequential request isolation using commodity Linux kernel features, and its integration into the OpenWhisk FaaS platform. Groundhog can be retrofitted to existing commercial systems without requiring any changes to existing functions, libraries, language runtimes, or OS kernels.

- ③ An experimental evaluation of Groundhog on functions from the FaaSProfiler, pyperformance, and PolyBench benchmarks within the OpenWhisk FaaS platform, which demonstrates that Groundhog provides sequential request isolation with low to modest overhead on function latency and peak throughput.

2 Background

Functions and Requests In the Function-as-a-Service (FaaS) model, tenants upload *functions* for execution by the cloud provider. A function is usually written in a high-level language, accepts input arguments, and returns results. The FaaS platform exposes an HTTP/S endpoint to which the tenant’s applications can send *requests* with arguments, and receive results in response.

Containers and Function Invocation The FaaS provider is responsible for executing functions on demand. FaaS platforms execute functions within *containers*, which may take the form of language-enforced compartments [13, 18, 40], processes [2], OS containers [6, 19, 31, 35], or virtual machines [1, 3]. When a request arrives for a particular function, an instance of the container needs to execute in order to serve the request. The FaaS platform may either instantiate a new container instance for the requested function from scratch—a *cold-start*—or *reuse* an existing idle container instance for the function if one exists.

FaaS platform services Many FaaS platforms offer tenant’s function implementations access to platform services. These services include storage, such as file access to scratch storage on a local disk, persistent key-value stores, or full relational database backends. Platform services may also provide automatic invocation of tenant’s functions triggered by timers, writes to certain key-value tuples, or updates to certain rows in a database.

Access control FaaS providers support client authentication on HTTP/S endpoints and minimally check if a caller is authorized to invoke the function, based on an access control list provided by the tenant.

Access to platform services by the function is controlled in this case on a per-tenant basis. Some FaaS providers like AWS-lambda, Azure FunctionApps, Google Cloud Functions, and IBM Cloud Functions [3, 19, 22, 31] associate more fine-grained, per-caller³ credentials to a function activation. Here, activations of the same function can have access to different platform services depending on the caller. Tenants can use this facility to control information flow via platform services among differently privileged callers of the same function, such as the different end-users of a tenant’s deployed application.

³In this paper, the caller is the entity causally responsible for the activation of a function.

Security vs. Performance Security is a chief concern – beyond per-tenant or per-caller access control to functions and platform services, FaaS platforms must prevent a buggy or malicious function from compromising other functions or obtaining unauthorized access to platform services. Containers are the key design choice for achieving such *function isolation*. Each container instance executes a single function. Moreover, a container may be reused for repeated invocations of the same function.

Sequential request isolation Our focus in this work is *sequential request isolation*, which isolates repeated invocations of the same function within the same container from each other. This isolation is important because bugs or compromises in a function implementation, or a third-party library or runtime the function relies on can cause confidentiality breaches by either (i) exposing private arguments of an activation to a subsequent activation of the function or (ii) using the credentials of an activation to obtain information from platform services and leak them to a subsequent, less privileged activation.

A trivial method of sequential request isolation is to start each request in a freshly-initialized container (forcing a cold-start on each request). However, container initialization is expensive, as is well-known from studies on FaaS cold start latencies. Despite excellent progress on reducing container initialization costs [5, 16, 45, 50], black-box techniques could still add hundreds of milliseconds of overhead on the critical execution path relative to standard insecure warm-container reuse. This overhead is of the same order of magnitude as a significant fraction of FaaS functions.

Consequently, we seek a different request isolation technique for FaaS that does not rely on container cold-start on every request and has minimal performance impact relative to an insecure baseline that provides no isolation between sequential requests to the same function. Our solution adds only a few milliseconds of overhead off the critical path of a request (median: 3.7 ms, 95p: 16.1 ms) and a minimal overhead for tracking modifications on the critical path (median: 1.5%, 95p: 7%) relative to an insecure baseline that does not provide sequential request isolation. We aim for a practical technique and particularly target a *black-box* approach that can be applied directly to functions independent of language or FaaS runtime.

3 Design Preliminaries

Groundhog operates at the level of OS processes. It can be readily integrated into FaaS platforms that encapsulate language runtimes and functions in processes or containers, which includes most major FaaS platforms currently in production use as far as we know. Moreover, Groundhog places no restrictions on function implementations or the programming language, runtime, and third-party libraries they rely on. Groundhog transparently interposes on API calls between a function implementation and the FaaS platform. Function implementations as well as the existing FaaS platform remain unchanged.



Fig. 1. Groundhog container life cycle

By interposing on a function’s API calls, Groundhog detects when the function is invoked and when its execution finishes and returns results. Groundhog uses this information to transparently create an initial snapshot of a newly created process and reverts its state after it has finished executing an invocation. For this purpose, Groundhog relies on a custom in-memory process snapshot/restore facility. The facility relies on standard Linux functionality, such as soft-dirty bits to track modified pages, the `/proc` filesystem to monitor changes to the process’ address space mappings and read/write process memory, and `ptrace` to orchestrate state snapshot and restore.

Fig. 1 illustrates a function process’s life cycle when Groundhog is being used. Groundhog avoids container, runtime, and data initialization steps when reusing a function container (process), and reverts the process’ state in a median of 3.7 ms (10p: 0.7 ms, 25p: 1 ms, 75p: 5.4 ms, 90p: 13 ms). From the perspective of the FaaS platform, the Groundhog-enabled container enjoys the benefits of container reuse, while ensuring sequential request isolation irrespective of bugs in a function’s implementation, libraries, or runtime.

3.1 Insights

Groundhog relies on two properties of the FaaS model as implemented by major FaaS platforms.

One-at-a-time function execution In FaaS platforms, each function container executes at most one request at a time. For scalable throughput, platforms create separate containers to concurrently execute activations of different functions or multiple activations of the same function.

Stateless functions In the FaaS programming model, a function implementation cannot expect that its internal state is retained across activations. To maintain persistent state, functions must instead rely on external or platform services such as a key-value store or a database backend.

Some FaaS platforms support *global state*, which can be initialized using a tenant-supplied script that is executed when a function container is initialized. Such an initialization step serves as mechanism to do operations or cache data that can be utilized by several activations regardless of their inputs (e.g., populating data structures, download machine learning models). This state is retained across invocations as long as the container is reused, but is lost when the FaaS platform shuts down a container. Since the platform is free to shut down a container at any time, functions must not rely on the persistence of global state for correctness.

These properties afford FaaS providers a high degree of flexibility in placing, scheduling, and dynamically replicating function activations. In the context of Groundhog, these properties imply that each reused container has well-defined points in its life cycle—namely between sequential activations—when

its state can be safely restored to a point after the initialization of global state but before the first function activation, thereby ensuring sequential request isolation.

Small write sets FaaS functions, particularly those written in managed languages, often use a substantial amount of memory, but only a small proportion of it is modified during an activation. This improves Groundhog’s efficiency because only modified parts of memory need to be restored after an activation. Our empirical evaluation on 58 benchmarks shows that the number of pages actually modified by each function invocation is only a small fraction of the overall function memory (mean: 8.5% of the mapped address space is modified, median: 3.3%, 90p: 17%). A similar observation was reported by REAP [45] where the examined functions’ working sets (both only read as well as modified pages) were on average 9% of their memory footprints.

3.2 Design options

Besides the trivial solution of using a fresh container for every request, which is inefficient, there are three broad design approaches for efficient sequential request isolation.

Language-based approaches When using appropriate safe programming languages [10], compiler instrumentation techniques [49], or runtimes [51] to implement functions, the language semantics can ensure efficient request isolation. However, this approach requires all tenants to use a particular (set of) programming languages/compiler, prevents the use of libraries written in unsafe languages for efficiency, and is vulnerable to bugs in the language runtime.

Fork A simple process-based technique is to fork a fully initialized function process, execute an activation within the child process, and discard the child process after the activation finishes. The main limitation of this approach is that fork as implemented in general-purpose operating systems cannot capture the state of a multi-threaded process. To take full advantage of container reuse, we need to be able to snapshot the fully initialized runtime of a managed language like JavaScript, which typically includes multiple active threads. Additionally, fork (or any copy-on-write (CoW) based approach) incurs expensive data-copying page faults during the execution of the function (i.e., on the critical path of a request).

Custom snapshot/restore facilities have been explored in prior work [5, 16, 24, 41, 42, 45] to reduce container cold-start costs by snapshotting an initialized runtime to disk/memory, and restoring it when a new container is needed. In principle, this approach could be used to instantiate a container for each activation. While substantially better than a cold-start for each activation, instantiating a container from a snapshot is still too expensive when compared to container reuse for many functions in our benchmarks.

3.3 Threat model

The FaaS platform, including the platform software, OS kernels, hypervisors, and platform services are trusted. We assume that the platform authenticates clients who connect to

HTTP/S endpoints, and enforces access control to functions, as well as a function activation’s access to platform services according to the authenticated client’s credentials.

Legitimate tenants are expected to set up access control lists that allow only legitimate parties to invoke their functions, and prevent unwanted information flow via platform services among legitimate callers with different privileges.

Function implementations provided by tenants, including any libraries they link and the language runtimes they rely on, are untrusted and may contain bugs. Under these assumptions, Groundhog prevents leaks of information from a function activation to subsequent ones, while allowing container reuse.

4 Groundhog Design

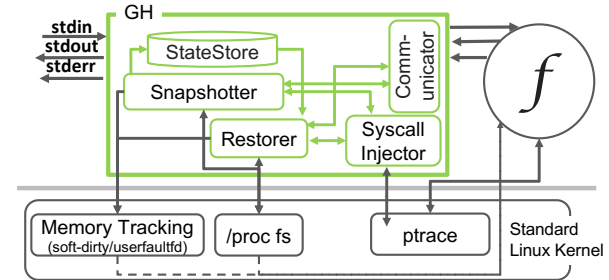


Fig. 2. Groundhog Architecture: (1) The manager (in green), (2) The function process. Groundhog relies on standard Linux kernel utilities.

Fig. 2 illustrates the Groundhog architecture. The Groundhog *manager* process (outermost green box) runs within an OS container alongside the function process, and is responsible for enforcing request isolation. Groundhog uses a novel, light-weight in-memory process snapshot/restore facility that achieves low restore times. The facility relies on standard Linux kernel facilities to snapshot, track, and restore processes. The design was guided by the following goals:

Generality The facility operates on a generic, multi-threaded POSIX process and does not make any assumptions about the function executing inside the process.

Restore cost proportional to modified pages To take advantage of the fact that most function activations only modify a small proportion of the function process’ state, Groundhog tracks which pages are modified during a function activation using the Linux soft dirty-bit facility. As a result, Groundhog need only restore modified pages after an activation.

Restore cost off the critical function execution path FaaS platform servers are less than fully utilized most of the time. Therefore, the design of Groundhog’s snapshot/restore facility seeks to minimize overhead *during* a function’s execution, in favor of performing all restore-related tasks *between* function activations. In particular, Groundhog avoids copy-on-write, which would burden function execution with expensive data-copying page faults. As a result, Groundhog avoids overhead on the end-to-end function execution latency in the common case of a less than fully utilized server.

4.1 Container initialization

The Groundhog manager process interposes between the FaaS platform and the process executing the function. The FaaS platform initializes the Groundhog manager process as if it were the process executing the function. The Groundhog manager then receives requests from the FaaS platform, relays them to the function process, and communicates results back to the FaaS platform. It communicates with the FaaS platform using the latter’s standard communication mechanisms (in OpenWhisk—the platform on which our prototype runs—these communication mechanisms are usually `stdin` and `stdout` pipes.)

To initialize the actual function process, Groundhog forks a new process, prepares pipes for communicating with it, drops privileges of the child process, and execs the actual function runtime in the child process.

Next, Groundhog creates a snapshot of the function process. For this, Groundhog invokes the function with *dummy* arguments that are independent of any client secrets (the dummy arguments are provided by the function deployer, once for every function they deploy, and can be part of the function’s configuration). After the function returns, it snapshots the state of the function process as described in §4.2. The purpose of the dummy invocation is to trigger lazy paging, lazy class loading and any application-level initialization of global state, and to capture these in the snapshot. Snapshotting without a dummy request would cause these (expensive) operations to happen again after every state restoration, which would increase the latency of subsequent function activations. This is particularly relevant when the function runs in an interpreted runtime like Python or Node.js, which heavily rely on lazy loading of classes and libraries [28].

After this snapshot is created, Groundhog informs the platform that it is ready to receive actual function invocation requests.

4.2 Snapshotting the function process

To take a snapshot, the manager interrupts the function process, then: (a) stores the CPU state of all threads using `ptrace` [25]; (b) scans the `/proc` file system to collect the memory mapped regions, memory metadata, and the data of all mapped memory pages; (c) stores all of this in the memory of the manager process; and (d) resets the soft dirty bit memory tracking state. Finally, the manager resumes the function process, which then waits for the first request inputs. Subsequently, Groundhog would restore the function’s process state back to this snapshot before each new request.

4.3 Tracking state modifications

Groundhog uses the standard *Soft-Dirty Bits* (SD) feature of the Linux kernel [26]⁴, which provides a page-granular, lightweight approach to tracking memory modifications. Each

⁴Available on stock Linux kernels v3.11+. We identified and reported a bug that affected the accuracy of the SD-Bits memory tracking in v5.6, it was fixed in v5.12 [32].

page has an associated bit (in the kernel), initially set to 0, that is set to 1 if the page is modified (dirtied). When a function invocation completes, Groundhog scans the SD-bits exposed by the Linux `/proc` filesystem to identify the modified pages. After restoring the function process, Groundhog resets all SD-bits to 0, ready for the next invocation.

We considered using Linux’s user-space fault tracking file descriptor (UFFD) [27]⁵ feature for memory tracking and prototyped this alternative; however we found UFFD to have significantly higher overhead compared to SD-bits due to the frequent context switches to user-space for fault handling.⁶ UFFD was faster than soft-dirty bits (and that too marginally) only when the number of dirtied pages was close to zero.

4.4 Restoring to the snapshotted state

When a function invocation completes, the function process returns the result to the Groundhog manager. Groundhog’s manager awaits the function response and forwards it to the FaaS platform (which then sends it to the caller). Next, the manager interrupts the function process and begins a restore. The manager identifies all changes to the memory layout by consulting `/proc/pid/maps` and `pagemap` (e.g. grown, shrunk, merged, split, deleted, new memory regions); these changes are later reversed by injecting syscalls using `ptrace` [25] (described below). The manager restores `brk`, removes added memory regions, remaps removed memory regions, zeroes the stack, restores memory contents of pages that have their SD-bit set, restores registers of all threads, madvises newly paged pages, and finally resets SD-bits.

To reverse memory layout changes, Groundhog injects system calls in the function process using `ptrace` [17, 25, 42]. After restoration completes, the child process is in an identical state to when it was snapshotted, and the process is ready to execute the next request. As an optimization, if a function within the same container is invoked consecutively by mutually trusting callers, then Groundhog can skip the rollback between such invocations.

4.5 Enforcing request isolation

Groundhog enforces request isolation by design. Groundhog prevents new requests from reaching the function’s process until it has been restored to a state free from any data of previous requests. This is achieved by intercepting the end-client requests before they reach the function and buffering them in Groundhog until the function’s process has been restored.

Although intercepting the communication ensures control of the function process and enforces security, it can add an overhead of copying request input/outputs to and from Groundhog’s manager process. This overhead can be eliminated as follows: (1) The FaaS platform can forward inputs directly to

⁵Write protection notifications available on stock Linux kernels v5.7+.

⁶A custom in-kernel facility that allows an application to request a list of modified pages presumably could be much faster, but would require kernel modifications.

the function process after waiting for a signal from Groundhog’s manager process that the function has been restored to a clean state. This requires minor, but trusted changes to the FaaS platform to wait for the signal from Groundhog. (2) Upon completion of a request, the function process can return outputs directly to the FaaS platform and, separately, signal Groundhog’s manager process that its state can be rolled back. The changes needed can be made in the I/O library that handles communication with the platform in the function process (no changes needed to the code of the individual functions submitted by the developers) and the changes do *not* have to be trusted for security – if the function process fails to signal Groundhog that it is done, Groundhog will never restore the state and will never signal the platform to send the next request.⁷

Design limitations: Groundhog does not currently allow function implementations to open arbitrary network connections and file descriptors. (None of the benchmarks we use in the evaluation require them.) Instead, functions are expected to rely on platform services for network communication and storage. Additionally, functions must externalize any caches whose state they wish to retain across requests since the state of in-address-space caches will be rolled back at every restore. Finally, as stated in our threat model, any external state (e.g. external storage, or the state of network connections and pipe contents) is assumed to be subject to access control. This is necessary to prevent data leaks across clients with different privileges via the external state.

5 Evaluation

In this section we evaluate Groundhog’s performance across a wide range of FaaS benchmarks. Overall, we show that:

- For a wide range of benchmark functions using three different languages/runtimes, Groundhog has modest overhead on end-to-end latency and throughput.
- Groundhog’s latency overhead depends primarily on the memory characteristics of the function and is proportional to the number of pages dirtied during a function’s execution. Groundhog’s throughput scales nearly linearly with the number of available cores.
- Groundhog’s lightweight restoration has equivalent or better performance than an alternative fork-based isolation approach, which is less general. We also compare to a WebAssembly-based isolation approach, and show that Groundhog has competitive performance despite being more general.

5.1 Evaluation Overview

Implementation. We implemented Groundhog in ~7K lines of C. Groundhog is compatible with off-the-shelf Linux and requires no kernel changes.

⁷We implemented (2) to facilitate debugging. Our evaluation still intercepts all inputs and outputs to demonstrate that platform modifications were not required and show the overhead of such interception on various functions.

OpenWhisk Integration. We integrated Groundhog with OpenWhisk [36], by modifying OpenWhisk’s container runtimes for Python and Node.js to include Groundhog. In addition, we implemented an OpenWhisk container runtime for native C, to enable the evaluation of native C FaaS benchmarks. Most OpenWhisk runtimes use the actionloop-proxy design, where a distinct process acts as a proxy that communicates with the OpenWhisk platform (through HTTP connections), and forwards the requests to the runtime process (through stdin) which has a simple wrapper to process inputs, call the developer’s function, and return results. Groundhog interposes between the proxy and the runtime, intercepting the stdin and stdout and forwards the stdin only when the function’s process is restored to a clean state. OpenWhisk’s container runtime for Node.js, on the other hand, is built using a single process that directly interacts with the platform and runs the function. We refactored it to an actionloop-proxy-like design to maintain a uniform Groundhog implementation that ensures security by blocking inputs until the function’s process is restored to a clean state⁸.

Hardware Configuration. We run all experiments on a private cluster hosting OpenStack/Microstack (ussuri, revision 233). Each physical host has an Intel Xeon E5-2667 v2 2-socket, 8-cores/socket processor, 256GB RAM and a 1 TB HDD.

OpenWhisk Deployment. We use the standard distributed Openwhisk deployment. Our distributed setup comprises 2VMs. One VM runs all OpenWhisk core components except for the invoker, which runs on a separate VM. The invoker is the component responsible for starting function containers locally and dispatching function requests to them; this is the component that interacts with and hosts Groundhog. We choose to isolate the invoker component in a separate VM to have more control on the variables affecting the experiments.

Both VMs are placed on the same physical host to minimize network communication overhead, creating favorable baseline conditions. To reduce potential performance interference, we pin the two VMs to separate cores and ensure that their memory is allocated from the corresponding NUMA domain. VMs are configured with 64GB RAM and an experiment-dependent number of cores (SMT turned off). The VMs run Ubuntu 20.04 with a stock Linux kernel v5.4. OpenWhisk is configured to run all functions with a 2GB RAM limit and a 5 minute timeout.

Experiment Configurations. To evaluate Groundhog’s overheads, we run two primary configurations: **BASE**, an insecure baseline using unmodified OpenWhisk that does not provide sequential request isolation (we prevent container cold-starts in our experiments to deliberately create an unfavorable but conservative baseline); and **GH**, which uses Groundhog on OpenWhisk to provide sequential isolation.

⁸Encapsulating the full process would require Groundhog to implement the platform API or have a small platform modification to allow blocking inputs until Groundhog signals to the platform that the function’s process is being restored as described in 4.5.

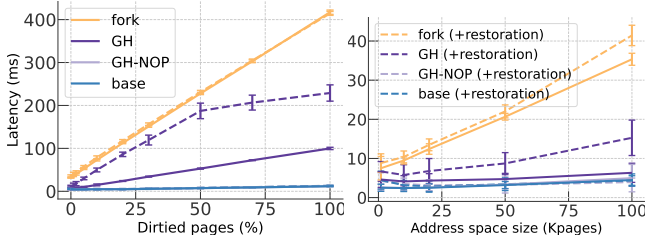


Fig. 3. Latencies varying the number of dirtied pages (left) and the address space size (right). Different colors represent different request isolation methods (or no isolation for BASE). Solid lines are latencies with in-function overhead but not restoration overhead, while dashed lines include both. (The lines of BASE and GH_{NOP} coincide visually in the figure.)

We also run a third configuration GH_{NOP} , which includes Groundhog but does not restore dirtied pages between consecutive invocations of the same function. This configuration represents an optimization for the case where consecutive requests are from the same security domain. The configuration also helps delineate Groundhog’s page tracking and restoration costs, which is the difference between the GH and GH_{NOP} configurations.

Lastly, we compare Groundhog to two alternative approaches. In §5.2.3 we implement a fork-based request isolation method, **FORK**, which is applicable to single-threaded applications and runtimes only. In §5.3.3 we compare Groundhog to **FAASM**, a research FaaS platform designed to reduce cold-start latencies for WebAssembly-compatible functions. We detail these alternative approaches in the respective sections.

5.2 Microbenchmarks

In this experiment, we evaluate Groundhog’s impact on request latency and how that impact varies with the memory size and the number of pages dirtied⁹. We evaluate both the *in-function* overheads that are on the critical path of function execution, and the *restoration overhead* which occurs off the critical path. We defer evaluating Groundhog’s snapshotting overheads, which occur only once after a new container starts, to §5.5.

Microbenchmark. We implement a simple function in C that pre-allocates an address space of a fixed size. Each invocation (a) dirties a subset of the pages by writing a word to each page of that subset, then (b) reads one word from each mapped page, even those that were not dirtied. We set up a 4-core VM with a single function-hosting container (this container is limited to 1 core), initialize the container, and then repeatedly invoke the function. We measure function latencies at the OpenWhisk invoker.

5.2.1 In-Function Overheads

Low-load Workload. We run the microbenchmark with a *low load* workload comprising 150 requests submitted one-at-a-time, with a small delay between consecutive requests. This

⁹We also considered address space fragmentation (same overall address space size but a varying number of memory maps) as an independent variable, but found that it has no statistically significant impact on the overhead of GH or FORK.

delay is sufficient for Groundhog to complete restoration before the next request arrives, so measurements for the low-load workload capture only the in-function overheads.

Results. The solid lines in Fig. 3 (left) plot function latency as we vary the percentage of pages dirtied from 0% to 100% with a fixed 100K mapped pages. As expected, GH introduces some latency overhead proportional to the number of dirtied pages. This overhead is due to a minor page fault to set the soft-dirty (SD) bit when a page is dirtied, which is required by the SD-bit mechanism on our hardware. In contrast, GH_{NOP} has negligible overhead relative to BASE since the SD-bits set in the first run are not reset (there is no memory restoration), and thus these page faults are not incurred in subsequent runs.

We also run a variant of the experiment where we fix the number of dirtied pages to 1K and vary the address space size from 1K to 100K pages. The solid lines in Fig. 3 (right) show the function latency as we vary the address space size. We observe that GH’s overhead is constant with respect to address space size because the in-function overheads depend only on the number of dirtied pages, which is fixed now.

5.2.2 In-function + Restoration Overheads

High-Load Workload. We repeat the two experiments above with a *high load* workload comprising 150 requests submitted back-to-back with no delay between consecutive requests. This leads to additional delays while waiting for Groundhog to complete restoration after the previous request. In contrast to the low-load workload, the high-load workload thus reflects *both* the in-function and the off-critical-path restoration overheads.

Results. The dashed lines in Fig. 3 (left) show the function latency as we vary the percentage of pages dirtied from 0% to 100% with a fixed 100K mapped pages. We observe higher latency overheads for the high-load workload (dashed lines) compared to the low-load workload (solid lines), and these overheads grow linearly as the percentage of dirtied pages increases. There is a change in slope at 60% because Groundhog is able to coalesce individual page restorations into fewer, larger memory copy operations, which are more efficient.

Next, we repeat the second experiment variant. Fig. 3 (right) shows the function latency as we vary the address space size from 1K to 100K pages while fixing the number of dirtied pages to 1K. Although in-function overheads are constant, restoration overheads in this experiment increase linearly with the address space size, because during restoration GH must scan the SD-bits of the whole address space to determine the pages to restore.

5.2.3 Comparison to Fork A potential alternative to our lightweight restoration is to use copy-on-write techniques such as fork (§3.2). Fork is not general purpose – it only works for single-threaded functions – however we provide a performance comparison for the purpose of illustration. We implement fork-based isolation and repeat the two microbenchmark experiments. In our fork-based implementation, we initialize the

function up to the same point where Groundhog takes its snapshot (a safe clean state). Instead of lightweight restoration, each request is then handled by a separate copy of the process forked at that state.

Fig. 3 (left) shows the function latency of FORK as we vary the percentage of pages dirtied from 0% to 100% with a fixed 100K mapped pages. We observe that the overhead of FORK is higher than GH because each page fault is significantly more expensive than for GH, entailing an additional page copy.

Fig. 3 (right) shows the function latency of FORK as we vary the address space size from 1K to 100K pages while fixing the number of dirtied pages to 1K. We see significantly higher overhead for FORK compared to Groundhog, and a linear increase in latency with the address space size. This increase is predominantly due to the additional overhead caused by dTLB misses on the first accesses to each page (even if unmodified) of the new process. This access can additionally require lazy creation of physical page table entries depending on the memory layout of the program.

5.3 FaaS Benchmarks

In this section we evaluate Groundhog’s impact on request latency and throughput for a range of FaaS benchmarks written in three different languages. We first compare Groundhog to an insecure baseline in OpenWhisk (§5.3.1). We then provide an illustrative comparison to a fork-based implementation (§5.3.2) and to FAASM, an alternative WebAssembly-based FaaS platform designed to optimize cold-starts, but that can also be used for request isolation in limited cases (§5.3.3).

Benchmarks. We evaluate 58 functions across three benchmarks and three languages: 22 python functions from the pyperformance benchmark [48], 23 C functions from PolyBench [30], and 13 functions (6 python, 7 Node.js) from the FaaSProfiler benchmark suite [38].

These functions cover a wide variety of real FaaS use cases such as Web applications, JSON and HTML parsing/conversion, string encoding, data compression, image processing (2D, 3D), optical character recognition (OCR), sentiment analysis, matrix computations (e.g. multiplication, triangular solvers), and statistical computations.

Latency. To measure latency we deploy a 4-core VM with a single function container that is limited to at most one core, and run a closed-loop client in a separate VM on the same machine¹⁰, which submits requests one-at-a-time. This workload is similar to the *low-load* setting from §5.2.1 and enables Groundhog to complete restoration in between consecutive requests, so latency measurements reflect Groundhog’s in-function overheads only. We report two latency measurements: the end-to-end latency of requests as experienced by the end-client (including all FaaS platform delays); and the invoker latency, which measures only the function execution time at

the invoker, excluding overheads of the remaining FaaS platform components, which Groundhog does not affect at all. All measurements are averages of 1,200 invocations, except for C functions longer than 10 seconds, where we report averages of 90 invocations.

Measuring Throughput. To measure throughput we deploy a 4-core VM with 4 function containers in a separate VM that maintains a large number of in-flight requests (both the number of function containers and in-flight requests are chosen empirically to maximize throughput). This workload is similar to the *high-load* setting from §5.2.2 as it ensures the FaaS platform is always saturated with requests. Throughput measurements thus account for Groundhog’s full overheads including both the in-function overheads and the restoration overheads. Unless otherwise specified, we report the peak sustained xput in 4 runs, each at least 1.5 minutes long.

Detailed Measurements. In addition to the figures presented in this section, full measurement data for our benchmarks can be found in Appendix A. Table 1 shows the absolute latency and throughput measurements for the BASE, GH, GH_{NOP}, FORK, and FAASM configurations. Table 2 shows the relative overheads compared to an insecure baseline. Table 3 shows the relation between the latency, overheads, and throughput of Groundhog.

5.3.1 Baseline Comparison Fig. 4 (a), (c) and (e) show the end-to-end request latency for all benchmarks. For each benchmark, we normalize the latency measurements relative to BASE; thus values <1 indicate better latency than the baseline and >1 represent worse latency.

We first consider the results for GH and GH_{NOP}. The main takeaway is that GH overhead on end-to-end latency relative to BASE is low overall. In most cases it is negligible (within one standard deviation). The median, 95th-percentile and maximum relative overheads are 1.5%, 7% and 54%, respectively, and the overhead is below 10.5% in all benchmarks except *img-resize(n)*, where it is 54.2% (discussed in the next paragraphs). The low overhead in most benchmarks is unsurprising, because end-to-end latency measurements include delays within the FaaS platform that are significant relative to the overhead added by the SD-bit tracking. These significant platform overheads are the same in the baseline and Groundhog.

GH overheads are more apparent when we inspect invoker latencies. Fig. 4 (b), (d) and (f) plot the invocation latency for all benchmarks, normalized to BASE. We observe that for python and C benchmarks the Groundhog overhead is relatively low. However, for some specific Node.js benchmarks (Fig. 4 (f), right) the overhead is more pronounced, up to 70% in the worst case. This occurs for two reasons.

First, GH proxies inputs to functions, which causes additional overheads for some of the Node.js functions with large inputs such as *json* and *img-resize* (which take inputs of 200kB and 76kB, respectively). This cost arises due to our refactoring of OpenWhisk’s Node.js runtime wrapper. This

¹⁰This placement minimizes network latencies to achieve best baseline performance and to allow easy and efficient scheduling of our 530 configurations on our resources.

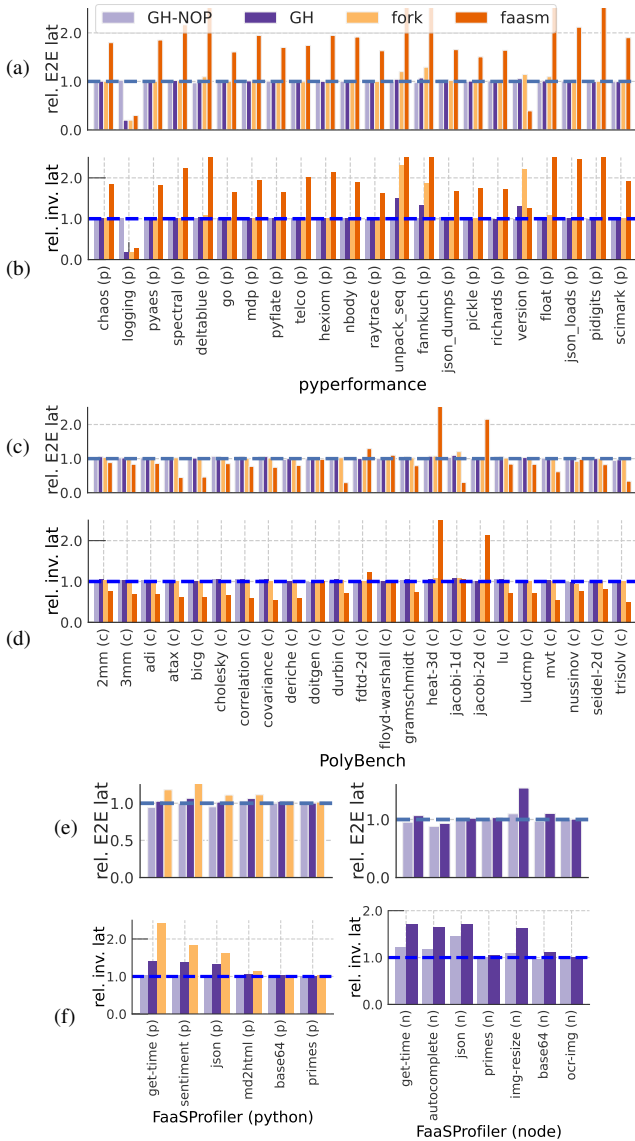


Fig. 4. Relative end-to-end latency and invoker-measured latency of GH, GH_{NOP}, FORK, and FAASM compared to the insecure baseline BASE. Figures are capped at 2.5X the baseline. Detailed numbers are in Appendix A. The symbols (p), (c) and (n) denote Python, C and Node.js benchmarks, respectively. **Lower numbers are better.**

overhead can be reduced by integrating Groundhog with the original single-process version of OpenWhisk Node.js.

Second, Node.js has a time-dependent behavior in garbage collection, namely, garbage collection can be triggered by the passage of time. Snapshotting and restoration can adversely affect this behavior, because restoration reverts the garbage collection state. The impact of this garbage collection was particularly pronounced on some benchmarks such as `img-resize(n)`. The problem can be alleviated by virtualizing time such that the process restoration resets the time to the original time of the snapshot, or by modifying the garbage collection in a time-independent way. This is actually a broader problem in the space of snapshot and restore techniques; a comprehensive

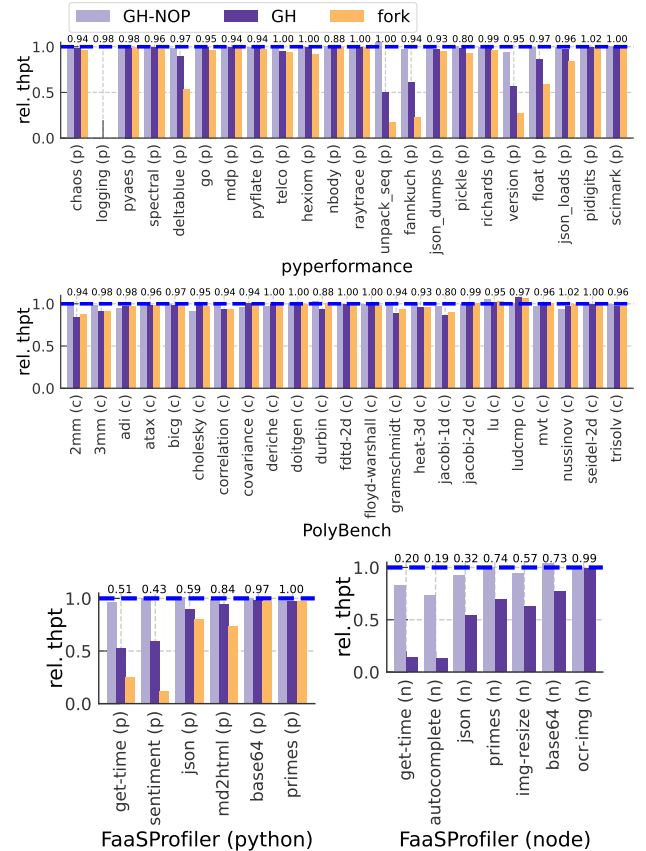


Fig. 5. Relative throughput of GH, GH_{NOP}, FORK compared to the insecure baseline BASE. Figures are capped at 2.5X the baseline. Detailed numbers are in Appendix A. The symbols (p), (c) and (n) denote Python, C and Node.js benchmarks, respectively. **Higher numbers are better.**

treatment of this topic is beyond the scope of this paper and left for future work.

Surprisingly, GH is faster than BASE on the benchmark `logging(p)`. We discovered that this occurred due to a memory leak in the function’s original implementation causing it to slow down after repeated invocations. GH’s restoration also rolls back the leaked memory, thus avoiding the slowdown.

Fig. 5 shows the request throughput for all benchmarks, normalized to BASE. Since functions are invoked sequentially, the throughput of GH relative to BASE should be inversely proportional to GH’s relative invoker latency, which is approximately $1 + (\text{in-function overhead} + \text{restoration overhead}) / (\text{baseline invoker latency})$. Our observations are consistent with this: The throughput plots in Fig. 5 show the reciprocal of this calculated number above each benchmark, and the heights of the GH bars are approximately equal to this reciprocal, as would be expected. For 40 out of 51 C and Python benchmarks the GH throughput is within 10% of BASE, and up to 50% lower on the remaining 11, mostly very short benchmarks. On Node.js benchmarks, where GH’s relative invoker latencies can be very high (as explained above), GH’s throughput is between 2% and 86% less than BASE’s. GH’s Node.js restoration overheads also

tend to be higher than other runtimes as Node.js’s runtime maps memory and performs memory layout changes aggressively (see Fig. 8 for the restoration overheads of specific benchmarks). Across all benchmarks, the median and 95th-percentile throughput reductions are 2.5% and 49.6%, respectively.

5.3.2 Comparison to Fork We also provide a comparison to the FORK alternative described in §5.2.3. Recall that fork is only applicable to single-threaded functions, thus we are unable to provide measurements for the Node.js runtime.

Fig. 4 also plots results for FORK for single-threaded benchmarks. The latency overhead of GH is slightly less than that of FORK since GH’s page faults are lighter than those of FORK (FORK’s page faults also require page copying, while GH’s page faults only set a SD-bit each).

Fig. 5 shows that the throughput of FORK follows a similar rule to that of GH. When compared to GH, FORK’s throughput is similar on all but very short benchmarks, where GH’s throughput is noticeably higher than FORK’s.

5.3.3 Comparison to Request Isolation using Faasm

A potential alternative to Groundhog’s process-based request isolation is to implement request isolation in the language runtime. To illustrate the performance trade-offs of the two approaches, we compare Groundhog to FAASM [40], a state-of-the-art FaaS platform where functions are isolated from each other not using OS containers but by compiling them to WebAssembly, and relying on spatial isolation within WebAssembly’s runtime. FAASM is designed to reduce FaaS cold-start latencies, but it can be used for efficient request isolation: WebAssembly limits each function to a *contiguous* 4GB memory map, which FAASM can quickly restore simply by a copy-on-write remapping after each request. Note that FAASM is not a fully general solution to the request isolation problem since it places restrictions on the functions – most notably, they must compile to WebAssembly.

FAASM comes with its own FaaS platform, which is significantly different from OpenWhisk. Despite the differences in the platforms, which make a direct comparison difficult, we compare Groundhog and FAASM for completeness sake. For the comparison, we use the pyperformance (python) and PolyBench (C) benchmarks, both of which can be compiled to WebAssembly as demonstrated in [40]. We rely on FAASM’s microbenchmarking infrastructure that reports both the overall latency (end-to-end and invoker) and the restoration (reset) cost.

Fig. 4 shows latencies for FAASM next to those for GH. On most pyperformance benchmarks, FAASM latency is considerably higher than that of GH, whereas the restoration time is comparable Fig. 6. This is because the Python interpreter and runtime are less efficient when compiled to WebAssembly (which FAASM uses) compared to a natively compiled interpreter (which GH uses).

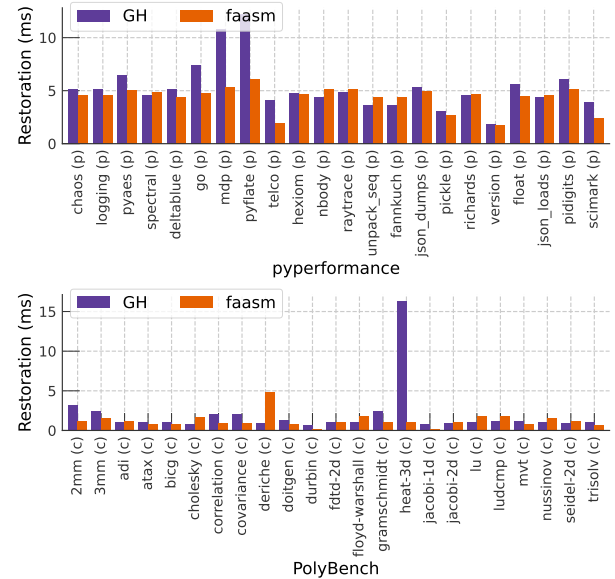


Fig. 6. Restoration duration (off the critical path) of GH, and FAASM. The symbols (p) and (c) denote Python and C.

On PolyBench functions, FAASM latencies are generally lower than those of GH. However, GH’s poorer relative performance are not because of Groundhog’s overheads. Rather, WebAssembly’s runtime is specifically optimized for program patterns that occur in PolyBench, so WebAssembly compiled PolyBench outperforms natively compiled PolyBench even in the baseline (this observation has been noted in prior work [21, 23, 40]).

The same trends continue to manifest in throughput measurements where FAASM has lower throughput than GH on most pyperformance functions, and higher throughput than GH on most PolyBench functions. We omit the detailed throughput comparison here as it entangles many variables such as the differences in the platforms, which have nothing to do with request isolation, the platforms’ internal components, runtimes (native vs WebAssembly), as well as the isolation mechanisms. The reader can find these numbers in Appendix A.

Overall, the performance differences between FAASM and GH are dominated by differences between native and WebAssembly compilation rather than request isolation costs.

5.3.4 Throughput scaling with cores

We expect GH’s throughput to scale linearly with cores as each core can run a completely independent container instance with its own function and Groundhog copy. To confirm this, we repeat the throughput experiment above, varying the number of cores available to the VM from 1 to 4 (and an equal number of function container instances, each limited to 1 core). Fig. 7 shows absolute throughputs as a function of the number of available cores for a subset of 14 representative benchmarks of varying duration, number of mapped pages and number of dirtied pages. Reported numbers are sustained throughputs averaged over 6 runs of at least 1.5 minutes each (excluding

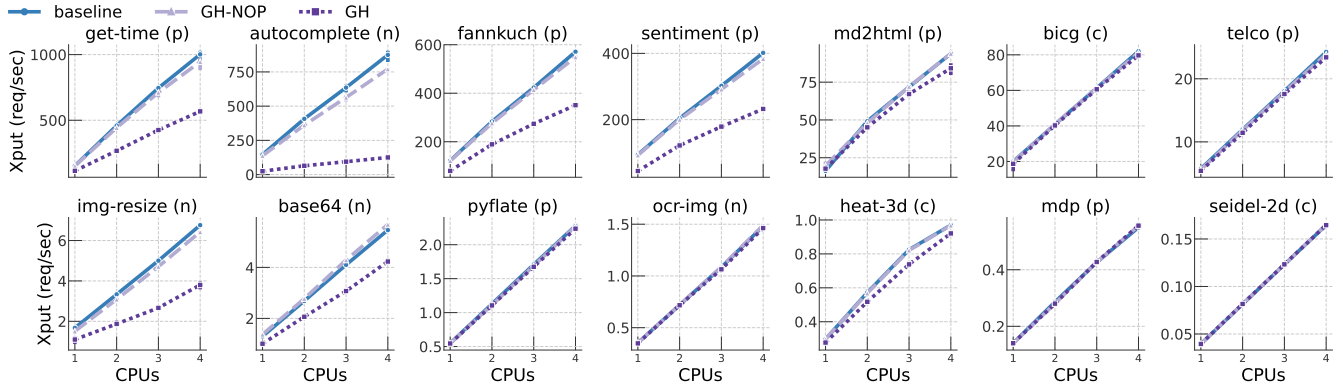


Fig. 7. Throughput scaling with number of cores on a subset of benchmarks

a warm-up). Error bars are standard deviations over the 6 runs. As expected, the scaling is nearly linear in all cases. We expect this nearly-linear trend to continue beyond 4 cores until a bottleneck in the kernel or memory buses arises.

5.4 Deconstructing restoration overheads

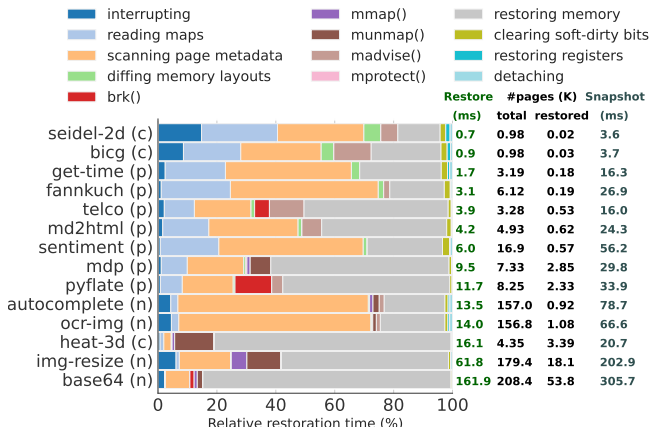


Fig. 8. Restoration overhead (deconstructed) and the one-time snapshotting overhead for a subset of benchmarks

Groundhog restoration involves several steps that we outlined in §4.4. In this section we break down the cost of restoration for the same 14 representative benchmarks (selection criteria in §5.3.4). The overall restoration cost breaks down into the following components:

- interrupting the function process.
- reading the process’ memory mapped regions
- scanning all mapped pages to identify which are dirtied
- diffing the memory layout to identify how it has changed
- restoring the original memory layout by injecting syscalls (brk, mmap, munmap, madvise, and mprotect)
- restoring the contents of modified and removed pages
- restoring registers
- resetting the soft-dirty bits of all modified pages
- detaching from the process

Each of these costs depends on different factors. The costs of interrupting, restoring registers, and detaching are functions of the number of threads in the process. The costs of reading, scanning, diffing the memory layout, and resetting soft-dirty bits, are functions of the address space size and layout. The syscall injection cost depends on the number of memory layout changes and is heavily dependent on the language runtime. Lastly, the cost of restoring the contents of pages depends on the number of pages dirtied during an invocation.

Fig. 8 shows these costs normalized to the total restoration cost for our 14 representative functions. For each benchmark we also detail the absolute restoration time, the number of pages, and the time for Groundhog to take its initial snapshot (we revisit snapshotting overhead in §5.5). In particular, we note that the memory restoration cost (■) is strongly correlated with the total number of pages restored. Similarly, the time spent scanning page metadata (■) is strongly correlated with the total number of pages (as discussed in §4.3, optimizations can make the costs correlate to the number of dirtied pages instead).

5.5 Snapshotting overhead

The rightmost column of Fig. 8 outlines Groundhog’s snapshotting latency overhead for the same 14 functions that we used in §5.3.4. Recall that snapshotting is a one-time operation that occurs upon container initialization. It involves warming the function by making a dummy request, pausing the process, and copying the process’s state to Groundhog’s manager process memory. Snapshotting time and memory costs are primarily proportional to the total number of paged memory pages. The snapshotting latency overhead can be alleviated using the same techniques that reduce cold start latencies (Catalyzer [16], REAP [45], FaaSnap [5], Replayable [50], Prebaking [41], Pagurus [24]) by checkpointing the initialized Groundhog process along with the function’s process. Groundhog memory overhead could be easily reduced to be proportional to the number of dirtied memory pages at the cost of a one-time on-critical-path copy-on-write per unique modified page in the

function’s life-cycle. Since snapshotting is an infrequent operation in Groundhog, we have not attempted these optimizations.

6 Related work

Fork-based request isolation A standard technique for request isolation in services, not FaaS specifically, is to fork a clean state to serve every request. For example, the Apache web server [7]¹¹ uses this approach to isolate client sessions from each other. The same idea can be used for request isolation in FaaS. However, `fork()` does not work with multithreaded functions or runtimes without extensive modifications to prepare all threads for a consistent snapshot [16]. Even for single-threaded functions, a fork-based approach is less performant than Groundhog (see §5) due to the high cost of the fork syscall and page-copying faults on the critical path for all written pages. The cost of fork itself can be reduced using lighter process-like abstractions such as lightweight contexts (lwCs) [29], but this does not reduce the cost of page copying on the critical path.

Advances in reducing container cold-start latencies Reducing container cold-start latencies is an active area of research. Several techniques have been proposed, including maintaining pre-warmed idle containers for a function [4, 8], maintaining a pool of containers that can be repurposed [33, 42], maintaining partially initialized runtimes with loaded libraries as in SOCK [34], relaxing isolation between functions by allowing functions from the same app developer to share containers (SAND [2], Azure [31]), and starting from slim container images and adding non-essential functions only when needed (CNTR [43]). These techniques do not provide request isolation, the problem that Groundhog targets, but they can be combined with Groundhog to solve the cold-start latency and the request isolation problems simultaneously.

Other methods of reducing cold-start latencies rely on snapshotting and restoration, which Groundhog also uses. Replayable [50] noted the phased nature of runtime initialization, so snapshotting after (part of) the initialization phase, and starting cold invocations from such a snapshot lowers cold-start latencies. In principle, this approach can also be used for request isolation by starting each invocation from such a snapshot but previous snapshot/restore techniques have overheads that are orders of magnitude higher than those of Groundhog.

Snapshotting techniques based on CRIU [12, 14, 15, 37, 46] serialize snapshots to persistent storage and are insufficient for request isolation due to the high overhead of deserialization during restoration, which is on the order of seconds.

Techniques that store snapshots in memory lower this overhead, but not sufficiently. For example, VAS-CRIU [47] treats the address spaces as a first-class OS primitive, allowing an address space to be attached to any process. However, container restoration time is still of the order of ~0.5s. SEUSS [11] takes

a unikernel approach, building a customized VM for each function where everything runs in kernel space. SEUSS allows incremental snapshots to jump-start functions. However, SEUSS (and VAS-CRIU) rely on copy-on-write, thus increasing the in-function latency, like the fork-based approach.

Catalyzer [16] trades function-start latency for in-function latency using a lazy restoration that incurs page faults. REAP [45] reduces the cost of these page faults by eagerly prefetching pages that were part of the active working set of the function in the past. However, overall function latencies after a restoration are still high: For a simple hello-world function that executes in 1ms without restoration, Catalyzer and REAP latencies with restoration are 232ms and 60ms, respectively. In contrast, Groundhog can restore a C hello world function in ~0.5 ms and an equivalent Python function in ~1.7 ms off the critical path.

FaaSnap [5] performs a different optimization – it enhances the pre-fetching of pages. For instance, it does concurrent prefetching while the VM is loading, and fetches pages in the approximate order of loading such that pages have a higher chance of being fetched by the time the function needs them. These optimizations further reduce the latency of cold-starts by 1.4x relative to a baseline without the optimizations. Nonetheless, overheads are high: The restoration of a simple hello world in FaaSnap takes as much time as it does in REAP.

Cloudflare Workers [13], Faastly [18, 44], and FAASM [40] solve the cold-start problem by relying on software-fault isolation (SFI) using V8 isolates and WebAssembly [51]. Here, several function spaces – called Faaslets in FAASM – are packed into a single running process, relying on SFI to isolate them from each other. Obtaining a fresh Faaslet for a function invocation amounts to remapping an unused Faaslet’s heap to a previously checkpointed, pre-warmed state of the function. WebAssembly limits the heap to a contiguous 4GB region, so this remapping is fast and effectively solves the cold-start problem. The FAASM paper notes that the same idea can be used for efficient request isolation by applying the remapping between requests. We compared the performance of this request isolation approach to that of Groundhog in §5 and showed that the trade-offs are very different. Unlike Groundhog, this technique is limited to languages, runtimes and threading models that can be compiled to WebAssembly.

7 Conclusion

Groundhog relies on efficient in-memory process state snapshot and restore to provide sequential request isolation in FaaS platforms. Groundhog’s design is agnostic to the FaaS platform, OS kernel, programming languages, runtimes, and libraries used to write functions. Groundhog overheads on end-to-end latency and throughput are modest, and lower than what could be achieved by repurposing state-of-the-art techniques for solving the container cold-start problem to provide sequential request isolation.

¹¹Using the default Apache Prefork MPM.

Acknowledgments

We thank Antoine Kaufmann, Akram El-Korashy, Vaastav Anand, Anjo Vahldiek-Oberwagner, Aastha Mehta, and the anonymous reviewers for their helpful feedback on earlier versions of this work. We thank Simon Shillaker for his help with reproducing FAASM results. This work was supported in part by the European Research Council (ERC Synergy imPACT 610150) and the German Science Foundation (DFG CRC 1223).

References

- [1] AGACHE, A., BROOKER, M., IORDACHE, A., LIGUORI, A., NEUGEBAUER, R., PIWONKA, P., AND POPA, D.-M. Firecracker: Lightweight virtualization for serverless applications. In *17th USENIX Symposium on Networked Systems Design and Implementation (NSDI 20)* (Santa Clara, CA, 2020), USENIX Association, pp. 419–434.
- [2] AKKUS, I. E., CHEN, R., RIMAC, I., STEIN, M., SATZKE, K., BECK, A., ADITYA, P., AND HILT, V. SAND: Towards high-performance serverless computing. In *2018 Usenix Annual Technical Conference (USENIX ATC 18)* (2018), pp. 923–935.
- [3] AMAZON AWS. AWS Lambda. <https://aws.amazon.com/lambda/>.
- [4] AMAZON AWS. Release: AWS Lambda on 2014-11-13. <https://aws.amazon.com/blogs/aws/new-provisioned-concurrency-for-lambda-functions/>, Accessed 24.11.2021.
- [5] AO, L., PORTER, G., AND VOELKER, G. M. Faasnap: Faas made fast using snapshot-based vms. In *Proceedings of the Seventeenth European Conference on Computer Systems* (2022), pp. 730–746.
- [6] APACHE. OpenWhisk. <https://openwhisk.apache.org/>.
- [7] APACHE. Apache MPM prefork. <https://httpd.apache.org/docs/2.4/mod/prefork.html>, Accessed 02.03.2021.
- [8] APACHE. Pre-Warmed actions in Openwhisk. <https://github.com/apache/openwhisk/blob/master/docs/actions.md/>, Accessed 24.11.2021.
- [9] AWS LAMBDA. Predictable start-up times with Provisioned Concurrency. <https://aws.amazon.com/blogs/compute/new-for-aws-lambda-predictable-start-up-times-with-provisioned-concurrency/>, Accessed 02.03.2021.
- [10] BOUCHER, S., KALIA, A., ANDERSEN, D. G., AND KAMINSKY, M. Putting the "micro" back in microservice. In *2018 USENIX Annual Technical Conference (USENIX ATC 18)* (2018), pp. 645–650.
- [11] CADDEN, J., UNGER, T., AWAD, Y., DONG, H., KRIEGER, O., AND APPAVOO, J. Seuss: skip redundant paths to make serverless fast. In *Proceedings of the Fifteenth European Conference on Computer Systems* (2020), pp. 1–15.
- [12] CHEN, Y. Checkpoint and restore of micro-service in docker containers. In *Proceedings of the 3rd International Conference on Mechatronics and Industrial Informatics* (2015/10), Atlantis Press, pp. 915–918.
- [13] CLOUDFLARE. Cloudflare Workers. <https://workers.cloudflare.com/>, Accessed 25.11.2021.
- [14] COOPERMAN, G., ANSEL, J., AND MA, X. Transparent adaptive library-based checkpointing for master-worker style parallelism. In *Sixth IEEE International Symposium on Cluster Computing and the Grid (CCGRID'06)* (2006), vol. 1, IEEE, pp. 9–pp.
- [15] CRIU. Checkpoint/Restore In Userspace. <https://www.criu.org/>, Accessed 03.12.2020.
- [16] DU, D., YU, T., XIA, Y., ZANG, B., YAN, G., QIN, C., WU, Q., AND CHEN, H. Catalyzer: Sub-millisecond startup for serverless computing with initialization-less booting. In *Proceedings of the Twenty-Fifth International Conference on Architectural Support for Programming Languages and Operating Systems* (2020), pp. 467–481.
- [17] EMPTYMONKEY. A ptrace library designed to simplify syscall injection in Linux. https://github.com/emptymonkey/ptrace_do, Accessed 03.12.2020.
- [18] FASTLY. <https://www.fastly.com/>. <https://www.fastly.com/>, Accessed 25.11.2021.
- [19] GOOGLE. Google Cloud Functions. <https://cloud.google.com/functions>, Accessed 12.01.2022.
- [20] GOOGLE CLOUD FUNCTIONS. Tips & Tricks for Cold Start). <https://cloud.google.com/functions/docs/bestpractices/tips>, Accessed 02.03.2021.
- [21] HAAS, A., ROSSBERG, A., SCHUFF, D. L., TITZER, B. L., HOLMAN, M., GOHMAN, D., WAGNER, L., ZAKAI, A., AND BASTIEN, J. Bringing the web up to speed with webassembly. In *Proceedings of the 38th ACM SIGPLAN Conference on Programming Language Design and Implementation* (2017), pp. 185–200.
- [22] IBM. IBM Cloud functions. <https://cloud.ibm.com/functions/>, Accessed 12.01.2022.
- [23] JANGDA, A., POWERS, B., BERGER, E. D., AND GUHA, A. Not so fast: Analyzing the performance of webassembly vs. native code. In *2019 USENIX Annual Technical Conference (USENIX ATC 19)* (2019), pp. 107–120.
- [24] LI, Z., CHEN, Q., AND GUO, M. Pagurus: Eliminating cold startup in serverless computing with inter-action container sharing. *arXiv preprint arXiv:2108.11240* (2021).
- [25] LINUX. ptrace – process trace interface. [https://man7.org/linux/man-pages/man2/ptrace.2.html/](https://man7.org/linux/man-pages/man2/ptrace.2.html), Accessed 21.04.2021.
- [26] LINUX. SOFT-DIRTY PTEs. <https://www.kernel.org/doc/Documentation/vm/soft-dirty.txt/>, Accessed 21.04.2021.
- [27] LINUX. Userfaultfd. <https://www.kernel.org/doc/html/latest/admin-guide/mm/userfaultfd.html>, Accessed 21.04.2021.
- [28] LION, D., CHIU, A., SUN, H., ZHUANG, X., GRCEVSKI, N., AND YUAN, D. Don't get caught in the cold, warm-up your JVM: Understand and eliminate JVM warm-up overhead in data-parallel systems. In *12th USENIX Symposium on Operating Systems Design and Implementation (OSDI 16)* (2016), pp. 383–400.
- [29] LITTON, J., VAHLIDIEK-OBERWAGNER, A., ELNIKETY, E., GARG, D., BHATTACHARJEE, B., AND DRUSCHEL, P. Light-weight contexts: An OS abstraction for safety and performance. In *12th USENIX Symposium on Operating Systems Design and Implementation (OSDI 16)* (2016), pp. 49–64.
- [30] LOUIS-NOEL POUCHET. Polybench/C). <http://web.cse.ohio-state.edu/~pouchet.2/software/polybench/>, Accessed 21.11.2021.
- [31] MICROSOFT. Azure Functions. <https://azure.microsoft.com/en-us/services/functions/>, Accessed 04.01.2022.
- [32] MOHAMED ALZAYAT. Detecting a bug in soft-dirty bits Kernel v5.6+. <https://lore.kernel.org/linux-mm/daa3dd43-1c1d-e035-58ea-994796df4660@suse.cz/T/>, Accessed 20.04.2021.
- [33] MOHAN, A., SANE, H., DOSHI, K., EDUPUGANTI, S., NAYAK, N., AND SUKHOMLINOV, V. Agile cold starts for scalable serverless. In *11th USENIX Workshop on Hot Topics in Cloud Computing (HotCloud 19)* (2019).
- [34] OAKES, E., YANG, L., ZHOU, D., HOUCK, K., HARTER, T., ARPACI-DUSSEAU, A., AND ARPACI-DUSSEAU, R. SOCK: Rapid task provisioning with serverless-optimized containers. In *2018 USENIX Annual Technical Conference (USENIX ATC 18)* (2018), pp. 57–70.
- [35] OPENFAAS. OpenFaaS. <https://www.openfaas.com/>, Accessed 12.01.2022.
- [36] OPENWHISK. OpenWhisk commit. <https://github.com/apache/openwhisk/commit/ed3f76e38d89468d11e862ee0539e74f02ac7f8e>.
- [37] RIEKER, M., ANSEL, J., AND COOPERMAN, G. Transparent user-level checkpointing for the native posix thread library for linux. In *PDPTA* (2006), vol. 6, pp. 492–498.
- [38] SHAHRAD, M., BALKIND, J., AND WENTZLAFF, D. Architectural implications of function-as-a-service computing. In *Proceedings of the 52nd Annual IEEE/ACM International Symposium on Microarchitecture* (New York, NY, USA, 2019), MICRO '52, Association for Computing Machinery, p. 1063–1075.

- [39] SHAHRAD, M., FONSECA, R., GOIRI, I., CHAUDHRY, G., BATUM, P., COOKE, J., LAUREANO, E., TRESNESS, C., RUSSINOVICH, M., AND BIANCHINI, R. Serverless in the wild: Characterizing and optimizing the serverless workload at a large cloud provider. In *2020 USENIX Annual Technical Conference (USENIX ATC 20)* (July 2020), USENIX Association, pp. 205–218.
- [40] SHILLAKER, S., AND PIETZUCH, P. FAASM: Lightweight isolation for efficient stateful serverless computing. In *2020 USENIX Annual Technical Conference (USENIX ATC 20)* (July 2020), USENIX Association, pp. 419–433.
- [41] SILVA, P., FIREMAN, D., AND PEREIRA, T. E. Prebaking functions to warm the serverless cold start. In *Proceedings of the 21st International Middleware Conference* (2020), pp. 1–13.
- [42] STENBOM, O. Refunction: Eliminating serverless cold starts through container reuse.
- [43] THALHEIM, J., BHATOTIA, P., FONSECA, P., AND KASIKCI, B. Cntr: Lightweight OS containers. In *2018 USENIX Annual Technical Conference (USENIX ATC 18)* (2018), pp. 199–212.
- [44] TYLER MCMULLEN (FASTLY). Lucet: A Compiler and Runtime for High-Concurrency Low-Latency Sandboxing. <https://popl20.sigplan.org/details/prisc-2020-papers/13/-Lucet-A-Compiler-and-Runtime-for-High-Concurrency-Low-Latency-Sandboxing>, Accessed 03.12.2020.
- [45] USTIUGOV, D., PETROV, P., KOGIAS, M., BUGNION, E., AND GROT, B. Benchmarking, analysis, and optimization of serverless function snapshots. In *Proceedings of the 26th ACM International Conference on Architectural Support for Programming Languages and Operating Systems (ASPLOS'21)* (2021), ACM.
- [46] VASAVADA, M., MUELLER, F., HARGROVE, P. H., AND ROMAN, E. Comparing different approaches for incremental checkpointing: The showdown. In *Linux Symposium* (2011), vol. 69.
- [47] VENKATESH, R. S., SMEJKAL, T., MILOJICIC, D. S., AND GAVRILOVSKA, A. Fast in-memory criu for docker containers. In *Proceedings of the International Symposium on Memory Systems* (2019), pp. 53–65.
- [48] VICTOR STINNER. The Python Performance Benchmark Suite). <https://pyperformance.readthedocs.io>, Accessed 21.11.2021.
- [49] VOGT, D., GIUFFRIDA, C., BOS, H., AND TANENBAUM, A. S. Lightweight memory checkpointing. In *2015 45th Annual IEEE/IFIP International Conference on Dependable Systems and Networks* (2015), IEEE, pp. 474–484.
- [50] WANG, K.-T. A., HO, R., AND WU, P. Replayable execution optimized for page sharing for a managed runtime environment. In *Proceedings of the Fourteenth EuroSys Conference 2019* (2019), pp. 1–16.
- [51] WEBASSEMBLY. WebAssembly). <https://webassembly.org/>.

A Detailed evaluation results

	E2E Latency (ms)	Invoker Latency (ms)	T'put (req/s)		E2E Latency (ms)	Invoker Latency (ms)	T'put (req/s)		E2E Latency (ms)	Invoker Latency (ms)	T'put (req/s)		E2E Latency (ms)	Invoker Latency (ms)	T'put (req/s)
base Gh Gh _{hp} fork faasm	(d)	class	beginning (p)	688 ±143	649 ±86	6.03	1288 ±657	1249 ±653	0.00	4707 ±99	4672 ±64	0.82	631 ±84	593 ±99	6.45
				691 ±111	652 ±39	5.94	259 ±68	228 ±52	16.3	4788 ±93	4751 ±61	0.80	642 ±87	605 ±14	6.40
				689 ±116	649 ±54	5.98	1319 ±648	1282 ±646	0.00	4734 ±100	4699 ±65	0.81	636 ±92	599 ±16	6.52
				690 ±105	651 ±64	5.81	260 ±73	224 ±48	15.6	4715 ±98	4678 ±53	0.81	638 ±83	602 ±13	6.24
1235 ±18	1201 ±13	2.99	383 ±12	345 ±26	9.69	8721 ±85	8559 ±73	0.40	8721 ±85	8559 ±73	0.40	1367 ±18	1323 ±5.1	2.62	
base Gh Gh _{hp} fork faasm	(p)	delahalle	go (p)	48.4 ±5.6	20.4 ±1.6	158	631 ±92	593 ±6.6	6.48	6377 ±88	6346 ±64	0.59	1636 ±76	1600 ±16	2.39
				50.3 ±5.2	21.3 ±2.0	140	637 ±110	597 ±5.7	6.42	6444 ±99	6412 ±82	0.58	1660 ±74	1623 ±13	2.34
				47.0 ±3.4	20.7 ±2.0	155	635 ±80	598 ±5.8	6.44	6395 ±103	6362 ±82	0.58	1645 ±69	1611 ±16	2.38
				53.0 ±5.5	22.1 ±1.9	84.7	634 ±84	596 ±6.4	6.24	6419 ±98	6387 ±81	0.58	1663 ±92	1623 ±11	2.32
150 ±5.8	129 ±2.1	24.4	1014 ±14	982 ±4.9	3.51	12422 ±105	12295 ±82	0.24	12422 ±105	12295 ±82	0.24	2780 ±30	2644 ±5.6	1.26	
base Gh Gh _{hp} fork faasm	(p)	telco	hexcom (p)	191 ±9.8	156 ±3.8	25.0	254 ±85	218 ±4.2	17.4	2859 ±96	2824 ±69	1.34	2496 ±107	2459 ±67	1.58
				191 ±7.3	158 ±3.0	23.8	254 ±84	219 ±4.0	17.3	2881 ±103	2845 ±53	1.34	2500 ±96	2464 ±51	1.57
				192 ±9.3	158 ±3.1	24.5	251 ±79	218 ±2.9	17.4	2869 ±90	2835 ±55	1.34	2494 ±80	2460 ±47	1.57
				189 ±7.1	157 ±3.6	23.4	255 ±72	220 ±3.7	16.0	2882 ±98	2847 ±60	1.33	2480 ±73	2458 ±44	1.56
332 ±9.9	315 ±0.7	11.3	495 ±10	467 ±1.6	7.60	5471 ±38	5361 ±2.6	0.63	5471 ±38	5361 ±2.6	0.63	4070 ±38	4001 ±4.0	0.83	
base Gh Gh _{hp} fork faasm	(p)	unpack_json	fannkuch (p)	28.3 ±2.1	3.33 ±1.2	802	29.7 ±2.5	4.59 ±1.2	572	567 ±7.6	533 ±6.0	7.19	139 ±80	106 ±1.9	35.5
				29.6 ±1.7	5.03 ±2.1	398	31.8 ±2.6	6.13 ±2.0	350	586 ±8.6	551 ±9.9	6.95	140 ±10.9	106 ±2.1	35.0
				28.4 ±2.2	3.44 ±1.4	836	29.0 ±1.6	4.70 ±1.5	557	586 ±10.1	549 ±8.2	7.11	139 ±69	105 ±1.8	35.4
				34.1 ±1.6	7.71 ±5.7	136	38.4 ±6.7	8.56 ±5.5	132	580 ±10.5	541 ±6.8	6.86	139 ±61	107 ±2.2	32.7
123 ±4.8	103 ±0.4	29.6	125 ±5.2	105 ±1.1	29.1	939 ±14	900 ±5.1	3.94	939 ±14	900 ±5.1	3.94	210 ±6.8	184 ±1.2	17.6	
base Gh Gh _{hp} fork faasm	(p)	richards	version (p)	387 ±7.7	353 ±4.6	10.7	28.2 ±2.3	3.07 ±1.6	990	57.3 ±6.5	27.1 ±1.9	126	135 ±8.2	102 ±1.9	36.5
				385 ±8.7	351 ±4.4	10.8	29.8 ±2.8	4.05 ±1.5	563	57.9 ±5.6	27.9 ±1.9	109	136 ±7.0	103 ±2.1	35.3
				391 ±11.2	353 ±6.2	10.6	27.9 ±2.7	3.03 ±1.2	925	56.2 ±5.1	27.1 ±1.9	125	136 ±7.3	103 ±2.1	36.3
				396 ±8.1	360 ±6.2	10.2	32.3 ±2.2	6.81 ±3.8	265	62.9 ±6.9	29.3 ±2.0	73.9	139 ±80	104 ±2.2	30.7
636 ±11	607 ±1.9	5.86	11.0 ±0.8	3.89 ±0.0	254	162 ±5.7	141 ±1.3	22.5	162 ±5.7	141 ±1.3	22.5	286 ±8.5	252 ±2.2	13.2	
base Gh Gh _{hp} fork faasm	(p)	pidigits	scmark (p)	2380 ±7.1	2348 ±5.8	1.64	1848 ±7.9	1813 ±3.1	2.12	27390 ±1548	27236 ±1544	0.12	45948 ±1849	45729 ±1717	0.07
				2380 ±5.6	2349 ±6.5	1.63	1841 ±7.5	1807 ±2.8	2.12	28963 ±1715	28887 ±1712	0.10	46901 ±2476	46824 ±2473	0.06
				2376 ±4.4	2347 ±5.6	1.64	1838 ±8.5	1801 ±2.8	2.14	28147 ±1908	28065 ±1906	0.13	47007 ±2714	46929 ±2716	0.07
				2385 ±5.9	2353 ±6.9	1.62	1868 ±7.7	1833 ±2.3	2.10	28274 ±2212	28183 ±2193	0.11	45736 ±2720	45661 ±2720	0.06
7224 ±4.4	6994 ±1.6	0.47	3513 ±2.5	3482 ±5.9	0.97	24181 ±2003	20590 ±2777	0.14	24181 ±2003	20590 ±2777	0.14	38270 ±3312	31627 ±2663	0.09	
base Gh Gh _{hp} fork faasm	(c)	ad	atx (c)	28470 ±1117	28311 ±923	0.12	68.7 ±6.4	36.5 ±1.6	93.5	75.9 ±7.5	42.8 ±1.9	81.0	16628.5 ±9224	16618.3 ±9209	0.02
				28941 ±1226	28858 ±1216	0.12	68.4 ±6.5	36.8 ±2.0	92.0	77.1 ±8.0	43.2 ±2.0	79.9	17580.3 ±8275	17569.2 ±8256	0.02
				29088 ±1156	29011 ±1152	0.11	70.6 ±7.5	36.5 ±1.7	93.1	75.7 ±7.5	42.7 ±1.8	80.6	17733.3 ±8313	17722.3 ±8310	0.02
				28257 ±1621	28173 ±1602	0.12	70.4 ±7.5	36.7 ±1.6	91.5	75.5 ±7.1	43.3 ±2.0	79.3	17072.8 ±11479	17062.9 ±11483	0.02
24456 ±2525	19504 ±1178	0.15	30.3 ±2.0	22.2 ±0.8	118	30.3 ±2.0	22.2 ±0.8	118	34.4 ±2.2	25.9 ±0.7	105	14025.9 ±21552	11243.0 ±8753	0.02	
base Gh Gh _{hp} fork faasm	(c)	correlatio	covariance (c)	32509 ±694	32430 ±693	0.10	33092 ±496	33021 ±495	0.10	1148 ±10.8	1115 ±8.6	4.47	691 ±10.1	651 ±1.5	5.98
				34406 ±1122	34329 ±1118	0.09	35055 ±1081	34971 ±1084	0.10	1148 ±10.4	1115 ±7.7	4.43	691 ±9.4	650 ±1.5	5.96
				34142 ±1038	34056 ±1029	0.10	34858 ±942	34776 ±948	0.10	1119 ±11.2	1086 ±9.0	4.34	688 ±11.8	646 ±1.3	6.01
				32964 ±987	32869 ±957	0.10	33715 ±1191	33641 ±1189	0.10	1146 ±11.4	1114 ±8.6	4.50	694 ±10.2	652 ±1.5	5.95
25082 ±3381	19377 ±4334	0.14	24674 ±3531	17964 ±4700	0.15	919 ±7.6	674 ±1.8	4.26	677 ±10.0	662 ±1.6	5.55				
base Gh Gh _{hp} fork faasm	(c)	dubbin	fld-2d (c)	33.1 ±2.7	7.64 ±1.4	315	2210 ±62	2179 ±24	0.89	21225 ±42	21151 ±39	0.17	61227 ±6114	60900 ±6020	0.06
				33.5 ±4.1	8.03 ±1.5	296	2213 ±58	2183 ±20	0.89	21243 ±39	21171 ±37	0.17	65076 ±2157	64980 ±2151	0.05
				32.0 ±1.9	7.65 ±1.1	325	34858 ±942	34776 ±948	0.10	21248 ±110	21158 ±44	0.17	62882 ±3330	62799 ±3331	0.06
				34.0 ±3.4	7.98 ±1.4	318	2209 ±60	2176 ±21	0.89	21234 ±66	21158 ±57	0.17	62591 ±1577	62507 ±1570	0.05
9.57 ±1.1	5.43 ±0.0	326	2856 ±24	2695 ±1.2	0.87	23356 ±165	21840 ±3.5	0.11	45304 ±2867	44627 ±2702	0.07				
base Gh Gh _{hp} fork faasm	(c)	heat-3d	jacob1-d (c)	3088 ±9.5	3060 ±8.2	1.02	27.9 ±1.8	3.81 ±1.2	671	2357 ±40	2329 ±1.7	1.05	196660 ±11451	196556 ±11445	0.02
				3305 ±6.6	3272 ±2.8	0.98	30.6 ±4.9	4.15 ±1.6	579	2378 ±76	2343 ±1.5	1.05	207712 ±13029	207604 ±13014	0.02
				3090 ±9.3	3060 ±7.3	1.02	28.9 ±4.2	3.87 ±1.2	652	2371 ±71	2338 ±1.7	1.04	206484 ±10894	206382 ±10885	0.02
				3319 ±4.8	3289 ±1.9	0.98	33.6 ±6.3	4.10 ±1.4	604	2368 ±63	2338 ±1.9	1.05	200061 ±11097	199953 ±11092	0.02
8780 ±4.9	8645 ±1.9	0.33	8.27 ±1.1	4.01 ±0.0	359	5077 ±57	4971 ±2.5	0.71	5077 ±57	4971 ±2.5	0.71	160516 ±4122	138303 ±6926	0.02	
base Gh Gh _{hp} fork faasm	(c)	ludcmp	mv (c)	193637 ±6461	193546 ±6466	0.02	176 ±8.7	140 ±3.1	28.8	39327 ±4277	39123 ±4053	0.09	23186 ±194	23140 ±22	0.16
				199649 ±8790	199550 ±8783	0.02	178 ±8.9	144 ±3.2	28.3	38398 ±830	38324 ±827	0.09	23173 ±46	23139 ±21	0.16
				199407 ±8662	199297 ±8660	0.02	179 ±8.1	145 ±3.6	28.0	38163 ±1059	38086 ±1058	0.08	23177 ±46	23142 ±20	0.16
				193763 ±6494	193653 ±6490	0.02	178 ±9.2	143 ±3.8	28.9	36208 ±1035	36134 ±1033	0.09	23180 ±51	23145 ±20	0.17
161293 ±3763	138991 ±10860	0.02	108 ±5.3	76.7 ±7.1	36.1	38477 ±3146	30232 ±1793	0.09	38477 ±3146	30232 ±1793	0.09	19062 ±88	18836 ±3.2	0.18	
base Gh Gh _{hp} fork faasm	(c)	trisolv	get-time (p)	57.6 ±7.5	23.1 ±1.5	138	29.6 ±3.4	2.94 ±1.2	1039	32.7 ±2.5	6.47 ±1.8	385	71.0 ±8.7	9.85 ±3.4	150
				55.8 ±6.5	23.2 ±2.2	135	30.4 ±3.5	4.15 ±1.7	552	34.9 ±3.4	8.88 ±3.2	230	72.1 ±7.3	13.0 ±4.0	135
				54.4 ±7.1	23.0 ±1.7	137	27.9 ±2.0	3.03 ±1.4	1004	32.6 ±2.7	6.64 ±1.8	385	67.6 ±7.7	10.0 ±3.4	152
				58.9 ±8.8	23.2 ±1.7	134	35.0 ±4.0	7.10 ±4.1	257	43.0 ±4.0	11.7 ±3.7	44.1	78.8 ±8.9	15.8 ±4.6	120
19.3 ±1.5	11.4 ±0.5	175													
base Gh Gh _{hp} fork faasm	(c)	m21hnl	p4mirc (n)	69.4 ±5.2	31.1 ±1.9	93.9	785 ±110	743 ±7.1	5.18	1867 ±89	1830 ±53	2.04	36.8 ±7.8	3.70 ±1.3	942
				73.8 ±7.5	32.7 ±2.3	88.5	806 ±107	761 ±10	5.10	1870 ±119	1831 ±75	1.99	39.3 ±8.7	6.37 ±3.6	133
				71.2 ±7.0	31.3 ±1.8	93.5	786 ±102	745 ±7.0	5.19	1860 ±105	1820 ±55	1.99	35.1 ±6.5	4.55 ±1.2	779
				77.2 ±6.2	35.1 ±2.4	68.8	807 ±100	764 ±9.3	5.05	1896 ±91	1857 ±35	1.99			
base Gh Gh _{hp} fork faasm	(c)	p4mirc	p4mirc (n)	42.7 ±11.1	3.82 ±1.4	923	71.1 ±10.1	9.39 ±3.5	159	317 ±10.9	275 ±2.0	11.8	506 ±132	445 ±7.4	6.57
				39.9 ±8.0	6.29 ±3.4	122	72.7 ±7.9	16.1 ±4.9	86.6	327 ±11.1	287 ±2.3	8.16	780 ±14.9	722 ±11.1	4.10
				37.7 ±8.2	4.47 ±1.3	677	72.5 ±8.9	13.6 ±3.6	147	319 ±10.1	279 ±2.0	11.8	556 ±14.8	491 ±6.8	6.18
base Gh Gh _{hp}	(n)	base64	octing (n)	686 ±10.7	644 ±2.0	5.62	2540 ±100	2492 ±1.1	1.53						
				758 ±11.2	715 ±2.1	4.34	2555 ±9.7								

Benchmark	Base End-to-End Latency (ms) / rel. overhead (%) \pm CoV(%)					Throughput (rfs) / rel. overhead (%)					Inv. lat (ms)/rel. (%) \pm CoV (%)		Restoration	
	baseline	GH-NOP	GH	fork	faasm	baseline	GH-NOP	GH	fork	faasm	baseline	GH	time (ms)	#Kpages (%)
chaos (p)	688.18±20.8	+0.12±16.8	+0.36±16.1	+0.22±15.3	+79.45±1.4	6.03	-0.90	-1.40	-3.70	-50.40	648.52±13.3	+0.54±6.0	4.9	0.47 (7.4)
logging (p)	1287.57±51.0	+2.43±49.1	-79.89±26.1	-79.82±28.3	-70.26±3.1	0	0	inf	inf	inf	1249.39±52.2	-81.76±2.3	4.8	0.41 (6.7)
pyaes (p)	4707.26±2.1	+0.57±2.1	+1.71±1.9	+0.16±2.1	+85.26±1.0	0.82	-0.40	-1.30	-1.00	-50.80	4671.98±1.4	+1.70±1.3	6	0.84 (13.5)
spectral (p)	630.84±13.4	+0.87±14.5	+1.84±13.6	+1.20±13.0	+116.72±1.3	6.45	+1.1	-0.80	-3.20	-59.30	592.76±1.7	+2.09±2.3	4.3	0.1 (21.4)
deltablue (p)	48.44±116.6	-2.97±71.6	+3.88±102.6	+9.51±103.8	+210.47±3.8	157.63	-1.70	-11.00	-46.30	-84.50	20.43±7.9	+4.33±9.5	4.6	0.33 (5.3)
go (p)	631.16±14.5	+0.32±12.7	+0.91±17.3	+0.41±13.2	+60.67±1.4	6.48	-0.60	-0.90	-3.60	-45.80	592.99±1.1	+0.61±1.0	6.9	0.95 (15.2)
mdp (p)	6377.46±1.4	+0.27±1.6	+1.05±1.5	+0.65±1.5	+94.77±0.8	0.59	-0.60	-1.00	-1.40	-58.80	6345.53±1.0	+1.05±1.3	9.6	2.85 (38.9)
pyflate (p)	1635.93±4.7	+0.53±4.2	+1.45±4.5	+1.65±5.5	+69.92±1.1	2.39	-0.60	-2.10	-3.20	-47.30	1599.84±1.0	+1.42±0.8	11.7	2.33 (28.2)
telco (p)	190.81±5.5	+0.80±48.2	+0.30±38.2	-0.83±37.3	+74.13±3.0	25.01	-2.00	-4.90	-6.50	-54.70	155.64±2.4	+1.54±1.9	3.9	0.53 (16.2)
hexiom (p)	253.92±33.5	-1.18±31.6	+0.13±33.2	+0.58±28.0	+94.80±2.1	17.45	-0.10	-1.00	-8.30	-56.50	218.21±1.9	+0.45±1.8	4.3	0.28 (4.5)
nbody (p)	2858.53±3.4	+0.38±3.1	+0.78±3.6	+0.83±3.4	+91.39±0.7	1.34	+0.0	-0.10	-0.70	-53.20	2823.65±2.4	+0.76±1.9	4.1	0.1 (21.4)
raytrace (p)	2495.66±4.3	-0.06±3.2	+0.17±3.8	-0.22±2.9	+63.10±0.9	1.58	-0.30	-0.60	-1.10	-47.60	2459.22±7.2	+0.19±2.1	4.4	0.35 (5.6)
unpack_seq (p)	28.34±74.3	+0.27±75.8	+4.45±56.3	+20.19±47.5	+333.81±3.9	801.86	+4.3	-50.40	-83.00	-96.30	3.32±36.8	+51.21±40.9	3.2	0.2 (3.3)
fannkuch (p)	29.7±83.6	-2.46±56.3	+7.04±83.3	+29.26±173.9	+319.97±4.2	572.32	-2.80	-38.80	-77.00	-94.90	4.59±27.1	+33.77±32.7	3.1	0.19 (3.1)
json_dumps (p)	567.41±13.3	+3.26±17.3	+3.19±14.6	+2.13±18.2	+65.41±1.5	7.19	-1.10	-3.40	-4.70	-45.30	533.09±1.1	+3.45±1.8	4.9	0.51 (8.0)
pickle (p)	139.26±57.7	+0.01±49.5	+0.64±77.5	-0.07±43.6	+50.49±3.2	35.49	-0.20	-1.40	-7.80	-50.60	105.64±1.8	+0.01±2.0	2.9	0.23 (6.7)
richards (p)	387.47±19.9	+1.01±28.7	-0.66±22.7	+2.22±20.4	+64.22±1.7	10.68	-0.50	+1.6	-4.10	-45.20	353.13±1.3	-0.56±1.3	4.2	0.23 (3.7)
version (p)	28.24±82.1	-1.35±98.6	+5.33±92.7	+14.34±66.8	-61.13±7.1	990.38	-6.60	-43.20	-73.30	-74.30	3.07±50.5	+31.82±36.0	1.7	0.17 (5.4)
float (p)	57.28±112.7	-1.80±90.7	+1.07±96.4	+9.73±110.0	+182.82±3.5	125.98	-0.80	-13.40	-41.30	-82.10	27.06±7.1	+2.91±6.7	5	0.65 (10.4)
json_loads (p)	135.04±60.7	+0.87±51.8	+1.04±51.2	+3.03±57.3	+111.67±3.0	36.46	-0.50	-3.20	-15.70	-63.70	101.98±1.9	+1.33±2.1	4	0.22 (6.3)
pidigits (p)	2380.0±0.3	-0.19±1.8	-0.01±2.4	+0.20±2.5	+203.53±0.6	1.64	-0.20	-0.50	-1.00	-71.50	2347.55±0.2	+0.07±0.3	5.4	0.81 (13.2)
scimark (p)	1848.12±4.3	-0.54±4.6	-0.37±4.1	+1.09±4.1	+90.08±0.7	2.12	+0.7	+0.0	-0.90	-54.40	1812.64±1.7	-0.34±1.6	3.8	0.52 (16.0)
2mm (c)	27390.28±5.7	+2.76±6.8	+5.74±5.9	+3.22±7.8	-11.72±12.0	0.12	+0.6	-16.10	-12.50	+10.7	27236.21±5.7	+6.06±5.9	3.1	0.02 (2.0)
3mm (c)	45947.69±4.0	+2.30±5.8	+2.07±5.3	-0.46±5.9	-16.71±8.7	0.07	-1.80	-8.80	-8.80	+23.4	45729.02±3.8	+2.40±5.3	2.3	0.02 (2.0)
adi (c)	28470.33±3.9	+2.17±4.0	+1.65±4.2	-0.75±5.7	-14.10±10.3	0.12	-5.80	-2.60	-2.80	+24.6	28311.08±3.3	+1.93±4.2	0.8	0.02 (2.0)
atax (c)	68.72±92.5	+2.78±105.9	-0.42±94.3	+2.52±106.4	-55.96±6.5	93.55	-0.50	-1.70	-2.20	+25.8	36.45±4.4	+1.01±5.4	1	0.03 (3.1)
bigc (c)	75.89±98.7	-0.20±98.5	+1.59±103.1	-0.45±93.9	-54.72±6.3	81.05	-0.50	-1.40	-2.10	+29.1	42.78±4.4	+0.89±4.7	0.9	0.03 (3.1)
cholesky (c)	166284.84±5.5	+6.64±4.7	+5.72±4.7	+2.67±6.7	-15.65±15.4	0.02	-8.60	-1.00	-2.60	+0.4	166182.88±5.5	+5.72±4.7	0.6	0.02 (2.0)
correlation (c)	32508.82±2.1	+5.02±3.0	+5.84±3.3	+1.40±3.0	-22.85±13.5	0.1	+2.4	-6.20	-5.90	+43.1	32429.64±2.1	+5.86±3.3	2	0.02 (2.0)
covariance (c)	33092.13±1.5	+5.34±2.7	+5.93±3.1	+1.88±3.5	-25.44±14.3	0.1	-3.80	+0.8	+0.4	+48.3	33020.56±1.5	+5.91±3.1	2	0.02 (2.0)
deriche (c)	1148.32±49.4	-2.56±10.1	-0.01±9.0	-0.16±9.9	-19.94±8.3	4.47	-3.00	-1.00	+0.6	-4.70	1114.99±7.7	+0.00±6.9	0.8	0.02 (2.0)
doitgen (c)	691.08±14.7	-0.44±17.1	-0.01±13.7	+0.45±14.8	-2.00±1.5	5.98	+0.6	-0.30	-0.40	-7.00	650.53±2.2	-0.08±2.3	1.3	0.02 (2.0)
durbin (c)	33.1±82.8	-3.25±59.5	+1.31±122.9	+2.64±100.6	-71.09±11.8	314.68	+3.2	-6.00	+1.0	+3.8	7.64±17.6	+5.05±18.4	0.6	0.02 (2.0)
fdtd-2d (c)	2209.61±2.8	+0.29±3.1	+0.15±2.6	-0.05±2.7	+29.23±0.9	0.89	-0.50	-0.30	+0.1	-2.30	2179.15±1.1	+0.16±0.9	1	0.02 (2.0)
floyd-warshall (c)	21224.8±0.2	+0.11±0.5	+0.09±0.2	+0.05±0.3	+10.04±0.7	0.17	-0.30	-1.80	-1.20	-35.20	21151.44±0.2	+0.09±0.2	0.8	0.02 (2.0)
gramschmidt (c)	61226.66±10.0	+2.70±5.3	+6.29±3.3	+2.23±2.5	-26.01±6.3	0.06	-1.10	-11.10	-6.20	+18.5	60899.77±9.9	+6.70±3.3	2.5	0.02 (2.0)
heat-3d (c)	3088.12±3.1	+0.07±3.0	+7.02±2.0	+7.47±1.5	+184.32±0.6	1.02	-0.40	-4.00	-4.10	-67.60	3059.55±2.7	+6.94±0.9	16.1	3.39 (77.9)
jacobi-1d (c)	27.92±63.9	+3.34±144.5	+9.65±159.4	+20.44±188.8	-70.39±12.8	671.34	-2.80	-13.80	-10.00	-46.60	3.81±32.7	+9.01±39.4	0.6	0.02 (2.0)
jacobi-2d (c)	2356.66±1.7	+0.62±3.0	+0.90±3.2	+0.49±2.7	+115.44±1.1	1.05	-0.20	0.00	+0.3	-32.10	2329.32±0.7	+0.60±0.6	0.7	0.02 (2.0)
lu (c)	196660.22±5.8	+5.00±5.3	+5.62±6.3	+1.73±5.5	-18.38±2.6	0.02	+5.8	+2.2	+3.3	+11.6	196555.78±5.8	+5.62±6.3	0.7	0.02 (2.0)
ludcmp (c)	193637.44±3.3	+2.98±4.3	+3.10±4.4	+0.06±3.4	-16.70±2.3	0.02	+0.1	+7.3	+7.0	+6.9	193545.91±3.3	+3.10±4.4	1	0.02 (2.0)
nvt (c)	176.37±49.5	+1.40±45.2	+0.89±49.9	+0.75±51.9	-38.62±4.9	28.78	-2.60	-1.70	+0.4	+25.3	140.33±2.2	+2.86±2.2	1.2	0.03 (3.1)
nussinov (c)	39326.91±10.9	-2.96±2.8	-2.36±2.2	-7.93±2.9	-2.16±8.2	0.09	-6.40	-3.00	-0.90	+2.0	39122.65±10.4	-2.04±2.2	1	0.02 (2.0)
seidel-2d (c)	23186.15±0.8	-0.04±0.2	-0.06±0.2	-0.02±0.2	-17.79±0.5	0.16	-0.50	+0.0	+0.6	+9.7	23140.14±0.1	-0.01±0.1	0.8	0.02 (2.0)
trisolv (c)	57.62±130.2	-5.65±130.4	-3.14±115.6	+2.28±149.3	-66.54±7.7	138.18	-0.80	-2.40	+2.80	+26.6	23.07±6.6	+0.42±9.3	1	0.02 (2.0)
get-time (p)	29.61±13.6	-5.68±72.6	+2.71±114.8	+18.13±114.1		1038.74	-3.30	-46.90	-75.30		2.94±40.5	+41.08±41.0	1.7	0.18 (5.6)
sentiment (p)	32.67±76.3	-0.10±82.0	+6.66±68.5	+31.69±92.4		385.07	0.00	-40.20	-88.50		6.47±27.2	+37.26±35.8	6	0.57 (3.4)
json (p)	70.97±122.9	-4.81±113.7	+1.56±101.8	+11.04±113.0		150	+1.5	-9.80	-19.80		9.85±34.2	+31.68±30.6	3.7	0.87 (26.1)
md2html (p)	69.36±75.3	+2.66±98.6	+6.36±101.6	+11.38±80.0		93.94	-0.50	-5.80	-26.80		31.04±6.3	+5.46±7.1	4.2	0.62 (12.6)
base64 (p)	785.33±14.0	+0.03±13.0	+2.63±13.3	+2.81±12.4		5.18	+0.2	-1.50	-2.50		743.23±1.0	+2.45±1.4	7.7	1.66 (32.4)
primes (p)	1866.58±4.8	-0.34±5.6	+0.17±6.3	+1.56±4.8		2.04	-2.40	-2.30	-2.40		1829.74±2.9	+0.05±4.1	3.2	0.53 (16.5)
get-time (n)	36.84±211.2	-4.69±184.6	+6.68±220.4			942.07	-17.30	-85.80			3.7±34.8	+72.22±56.2	12.6	0.64 (0.4)
autocomplete (n)	42.74±260.6	-11.90±217.9	-6.71±201.2			922.59	-26.60	-86.80			3.82±36.8	+64.58±54.2	13.5	0.92 (0.6)
json (n)	71.1±142.4	+1.99±122.7	+2.22±108.5			159.09	-7.50	-45.60			9.4±37.8	+71.32±30.7	13	0.85 (5.0)
primes (n)	316.85±34.3	+0.65±31.7	+3.27±33.9			11.79	+0.1	-30.70			274.63±7.3	+4.56±8.0	84.7	34.2 (17.0)
img-resize (n)	505.76±26.0	+9.87±26.6	+54.20±19.2			6.57	-6.00	-37.60			445.27±16.7	+62.09±15.3	61.8	18.05 (10.1)
base64 (n)	686.33±15.6	-3.19±17.8	+10.48±14.7			5.62	+4.1	-22.80			644.02±3.1	+11.04±2.9	161.9	53.83 (25.8)
ocr-img (n)	2539.62±3.9	+0.43±4.2	+0.60±3.8			1.53	-0.40	-1.00			2491.66±0.4	+0.68±0.5	13.9	1.08 (0.7)

Table 2. Latency and throughput measurements showing the overheads of GH_{no} (Groundhog with no restoration), GH_{fork}, and FAASM relative to an unsecure baseline. We run 58 benchmarks across three languages indicated by (p) python, (c) c, and (n) Node.js. We highlight cells of interest if there is more than a 5% difference as follows: **Green** indicates results favorable to Groundhog **Red** indicates results unfavorable to Groundhog **Blue** indicates the unexpected result that Groundhog is outperforming the baseline. GH’s impact on throughput can be approximated by the relative restoration time compared to the invoker’s latency (inv. lat.). **Disclaimer:** Faasm throughput measurements are provided for the curious reader, but no conclusions should be drawn based on them as they entangle many variables such as the difference in the platforms, their internal components and deployment, runtimes (native vs WebAssembly), as well as the isolation mechanism

<i>Benchmark</i>	<i>baseline</i>		<i>Groundhog</i>		<i>Restoration</i>			
	Invoker lat (ms)	T'put	Invoker lat (ms)	T'put	time (ms)	#pages (K)	#faults (K)	#restored (K)
cholesky (c)	166182.8±9208.73	0.02	175691.9±8256.49	0.02	0.57	0.98	0.02	0.01
jacobi-1d (c)	3.8±1.25	671.34	4.2±1.64	578.99	0.62	0.98	0.03	0.02
durbin (c)	7.6±1.35	314.68	8.0±1.48	295.98	0.62	0.98	0.03	0.02
jacobi-2d (c)	2329.3±17.03	1.05	2343.4±14.98	1.05	0.69	0.98	0.02	0.01
lu (c)	196555.8±11445.0	0.02	207603.5±13014.02	0.02	0.74	0.98	0.02	0.01
seidel-2d (c)	23140.1±22.03	0.16	23139.0±21.4	0.16	0.75	0.98	0.02	0.02
deriche (c)	1115.0±86.2	4.47	1115.0±76.95	4.43	0.75	0.98	0.02	0.01
adi (c)	28311.1±923.24	0.12	28857.6±1215.98	0.12	0.77	0.98	0.02	0.02
floyd-warshall (c)	21151.4±39.35	0.17	21171.3±37.12	0.17	0.78	0.98	0.02	0.01
bicg (c)	42.8±1.88	81.05	43.2±2.03	79.87	0.93	0.98	0.03	0.03
fdtd-2d (c)	2179.1±23.85	0.89	2182.6±19.73	0.89	0.97	0.98	0.02	0.02
trisolv (c)	23.1±1.51	138.18	23.2±2.16	134.92	0.97	0.98	0.03	0.02
atax (c)	36.4±1.6	93.55	36.8±1.99	91.99	0.99	0.98	0.03	0.03
nussinov (c)	39122.6±4053.11	0.09	38323.5±827.3	0.09	1.02	0.98	0.02	0.02
ludcmp (c)	193545.9±6455.96	0.02	199550.2±8782.81	0.02	1.02	0.98	0.03	0.02
mvt (c)	140.3±3.06	28.78	144.3±3.2	28.28	1.16	0.98	0.04	0.03
doitgen (c)	650.5±14.61	5.98	650.0±14.79	5.96	1.31	0.98	0.04	0.02
version (p)	3.1±1.55	990.38	4.0±1.46	562.89	1.66	3.14	0.17	0.17
get-time (p)	2.9±1.19	1038.74	4.1±1.7	552.09	1.66	3.19	0.18	0.18
covariance (c)	33020.6±494.9	0.10	34971.3±1084.18	0.10	1.97	0.98	0.04	0.02
correlation (c)	32429.6±692.85	0.10	34328.9±1118.18	0.09	2.00	0.98	0.04	0.02
3mm (c)	45729.0±1717.42	0.07	46824.4±2473.21	0.06	2.32	0.98	0.04	0.02
gramschmidt (c)	60899.8±6020.33	0.06	64980.4±2150.99	0.05	2.53	0.98	0.04	0.02
pickle (p)	105.6±1.89	35.49	105.7±2.11	34.98	2.90	3.45	0.23	0.23
2mm (c)	27236.2±1544.4	0.12	28887.4±1712.35	0.10	3.12	0.98	0.04	0.02
fannkuch (p)	4.6±1.24	572.32	6.1±2.0	350.22	3.14	6.12	0.19	0.19
unpack_seq (p)	3.3±1.22	801.86	5.0±2.06	398.15	3.17	6.12	0.20	0.20
primes (p)	1829.7±53.45	2.04	1830.7±75.43	1.99	3.24	3.22	0.51	0.53
json (p)	9.9±3.37	150.00	13.0±3.97	135.34	3.71	3.33	0.64	0.87
scimark (p)	1812.6±30.71	2.12	1806.6±28.47	2.12	3.77	3.26	0.51	0.52
telco (p)	155.6±3.8	25.01	158.0±2.95	23.77	3.91	3.29	0.53	0.53
json_loads (p)	102.0±1.95	36.46	103.3±2.14	35.29	4.04	6.12	0.22	0.22
nbody (p)	2823.7±69.0	1.34	2845.0±53.46	1.34	4.08	6.12	0.21	0.21
richards (p)	353.1±4.64	10.68	351.1±4.41	10.85	4.16	6.18	0.23	0.23
md2html (p)	31.0±1.95	93.94	32.7±2.31	88.50	4.25	4.93	0.63	0.62
spectral (p)	592.8±9.92	6.45	605.2±14.14	6.40	4.29	6.12	0.22	0.21
hexiom (p)	218.2±4.21	17.45	219.2±3.98	17.28	4.35	6.18	0.28	0.28
raytrace (p)	2459.2±67.26	1.58	2463.9±51.19	1.57	4.42	6.25	0.36	0.35
deltablue (p)	20.4±1.61	157.63	21.3±2.02	140.26	4.64	6.18	0.23	0.33
logging (p)	1249.4±652.55	0.00	227.9±5.2	16.34	4.77	6.12	0.42	0.41
json_dumps (p)	533.1±6.0	7.19	551.5±9.92	6.95	4.92	6.37	0.51	0.51
chaos (p)	648.5±86.06	6.03	652.0±39.21	5.94	4.93	6.32	0.47	0.47
float (p)	27.1±1.92	125.98	27.8±1.87	109.09	4.99	6.26	0.65	0.65
pidigits (p)	2347.6±5.76	1.64	2349.1±6.51	1.63	5.40	6.14	0.81	0.81
sentiment (p)	6.5±1.76	385.07	8.9±3.18	230.39	6.00	16.86	0.57	0.57
pyaes (p)	4672.0±63.68	0.82	4751.3±61.36	0.80	6.02	6.21	0.83	0.84
go (p)	593.0±6.64	6.48	596.6±5.69	6.42	6.90	6.25	0.84	0.95
base64 (p)	743.2±7.11	5.18	761.5±10.48	5.10	7.67	5.13	1.86	1.66
mdp (p)	6345.5±63.96	0.59	6412.3±82.13	0.58	9.55	7.33	2.22	2.85
pyflate (p)	1599.8±16.39	2.39	1622.5±12.58	2.34	11.67	8.25	3.01	2.33
get-time (n)	3.7±1.29	942.07	6.4±3.58	133.45	12.58	156.76	0.59	0.64
json (n)	9.4±3.55	159.09	16.1±4.94	86.58	13.02	156.78	0.67	0.85
autocomplete (n)	3.8±1.41	922.59	6.3±3.41	121.98	13.52	156.98	0.69	0.92
ocr-img (n)	2491.7±10.63	1.53	2508.5±12.24	1.52	13.95	156.80	0.89	1.08
heat-3d (c)	3059.5±81.59	1.02	3272.0±28.01	0.98	16.09	4.35	0.02	3.39
img-resize (n)	445.3±74.34	6.57	721.7±110.76	4.10	61.83	179.43	9.58	18.05
primes (n)	274.6±20.11	11.79	287.1±23.1	8.16	84.74	201.35	1.27	34.20
base64 (n)	644.0±20.22	5.62	715.1±20.89	4.34	161.93	208.42	47.98	53.83

Table 3. Groundhog’s overhead on the throughput is a function of Groundhog’s added overhead both on the critical path (#faults) which has negligible overhead on most functions, as well as the overhead off the critical path (Restoration time) which is mostly a function of the address space size (#pages (K)) and the number of restored pages (#restored (K)) as well as restoring the memory layout as demonstrated earlier in Fig. 8. Data is sorted by the restoration time.